■ Interagency Ecological Program for the San Francisco Estuary ■

IEP NEWSLETTER

VOLUME 19, NUMBER 3, Summer/Fall 2006

Of Interest to Managers 2

IEP Quarterly Highlights 3

Delta Water Project Operations 3

Fish Conservation and Culture Lab (FCCL), Fall 2006 6

Status and Trends 6

Common Shrimp of the San Francisco Estuary - 2004 Status and Trends Report 6

Fish Salvage at the State Water Project and Central Valley Project Fish Facilites in 2004 10

Contributed Papers 17

Estimating Dissolved Inorganic Carbon Concentration from Salinity in San Francisco Bay for Use in ^{14}C-Primary Production Studies 17

The Vertical Structure of Dissipation in Tidally-Forced Shallow Water Body with Locally Generated Waves 22

■

Of Interest to Managers

Ted Sommer (DWR), tsommer@water.ca.gov

This issue's Quarterly Highlights includes updates on Delta water project operations, delta smelt hatchery work, status and trends of estuarine shrimp, and salvage at the SWP and CVP fish facilities. Kate Le's review of Delta water project operations indicates that heavy precipitation during and winter and spring 2006 resulted in relatively high outflow conditions during the remainder of the water year. Theresa Rettinghouse's update for the UCD Fish Conservation and Culture Lab reflects ongoing efforts to improve production efficiency of young delta smelt, now critical for many laboratory and field studies of this threatened fish. Kathy Hieb's review of trends in estuarine shrimp reveals that populations of several of these crustaceans remain relatively robust. In general, these shrimp do not show evidence of the major collapse reported for pelagic fishes. The article includes an update on the recent invasion by a the Siberian prawn, *Exopaleomon modestus*, which now occurs upstream to Knights Landing on the Sacramento River, and to Mud Slough on the San Joaquin River. Russ Gartz's Quarterly Highlight is an update through 2004 of trends in salvage data at the fish facilities of the two water projects, the SWP and CVP. The results are consistent with long-term patterns that salvage trends vary seasonally and annually, and differ substantially for each species. A positive sign for operations is that Chinese mitten crabs, a nuisance species at the fish facilities, continue to decline in numbers at the SWP and CVP.

Alex Parker's Contributed Paper focuses on efforts to improve measurements of dissolved inorganic carbon, one of the variables needed to estimate primary production, a measure of the base of the food web. Parker has developed an equation based on salinity that will simplify future studies on primary production in the San Francisco Estuary.

This issue of the IEP Newsletter concludes with an article about measurements of the hydrodynamics of a shallow bay. Nicole Jones' results demonstrate the need to consider wind-generated turbulence in current hydrodynamic models, a tool now widely-used for research and management in the San Francisco Estuary. Examples where this issue could be important include analyses of transport and mixing of sediment and organisms (e.g. phytoplankton).

IEP QUARTERLY HIGHLIGHTS

DELTA WATER PROJECT OPERATIONS

Kate Le (DWR), kle@water.ca.gov

April - June

During the April through June 2006 period, both the Sacramento River and San Joaquin River flows were unusually high due to high runoffs from previous months and continued precipitation in the early half of April as shown in Figure 1. Sacramento flows ranged between 640 cms (22,600 cfs) and 2,700 cms (95,340 cfs). San Joaquin flows ranged between 390 cms (13,770 cfs) and 1,000 cms (35,310 cfs). As a result of these high river flows, NDOI was extremely high too. NDOI flows ranged between 750 cms (26,480 cfs) and 7,000 cms (247,175 cfs). Most of the high flows occurred in April then gradually declined thereafter as a result of VAMP and minimal precipitation activity. At the end of June, all flows almost converge below 1,000 cms (35,310 cfs) as shown in Figure 1.

Meeting hydrology or water quality standards was not a concern during this period or for the entire year because of the wet hydrologic conditions in the Delta which resulted from heavy rains in the early part of 2006. Unlike previous years, April through June 2006 export actions at SWP and CVP were operated primarily for VAMP (Figure 2). The following is a monthly summary of the reasons for the operational actions at both water projects during this period.

- April 2006: San Luis filled to capacity and pumping rates at both water projects were to meet demands.
- May 2006: Both water projects operated for VAMP. The first 15 days combined pumping held at about 43 cms (1,500 cfs) and the last 15 days combined pumping increased, but was held to about 170 cms (6,000 cfs).
- June 2006: At the beginning of June, SWP reduced pumping for herbicide treatment of aquatic plants. On June 7, SWP was reduced for fish concerns (fall and spring-runs). On June 21, CVP was reduced due to a malfunction.

July - September

During the July through September 2006 period, San Joaquin River flow ranged between 76 and 370 cubic meters per second (2,700 cfs and 13,000 cfs), Sacramento flow ranged between 428 and 637 cubic meters per second (15,100 cfs to 22,486 cfs). The Net Delta Outflow Index (NDOI) ranged between 180 and 670 cubic meters per second (6,300 cfs and 23,470 cfs) as shown in Figure 3. The flow decrease in early July along San Joaquin River was a result of reduced releases. NDOI flows also responded to this reduction as shown in Figure 3. Sacramento River releases were reduced as well, but at a more gradual step. Despite all the upstream flow reductions, the overall flow range was higher than the previous year, and is probably due to the continued carry over effect of high flows from the storms in the early half of 2006. Typically, flow patterns after mid-August are controlled by either outflow or water quality standards. However, this year Sacramento, San Joaquin, and outflow index levels were maintained at a flow range that was sufficient enough not to trigger any standards.

Export rates during the July through September 2006 period were stable for the most part for both water projects. CVP pumping was about 125 cubic meters per second, whereas SWP pumping was about 200 cubic meters per second, except during mid-July(Figure 4). The reduced pumping in mid-July was to maintain water levels for siphons drawing agricultural water in the south Delta. Thereafter, SWP pumping was primarily for an additional 500 cfs for EWA since the export to inflow ratio standard was 65%. In past years, water quality would be controlled by regulated inflows and exports during this time period; however, there were no standards triggered during this period, as a result of wet conditions in early 2006.

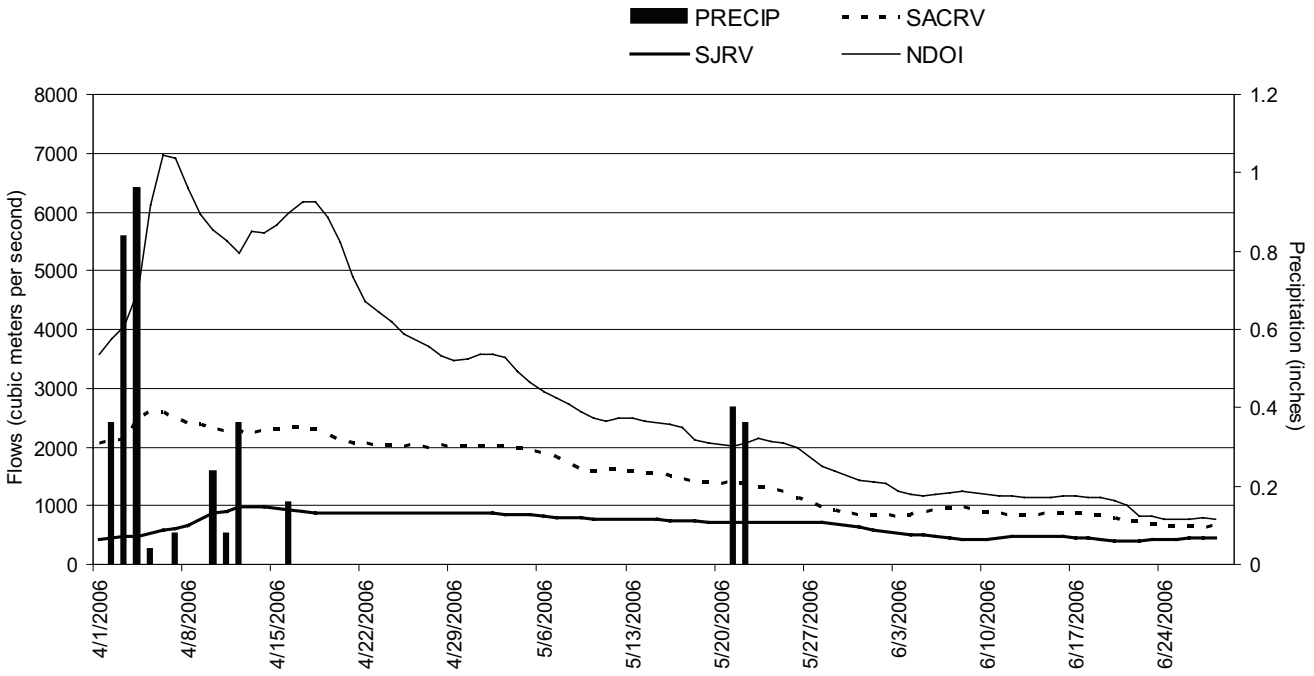

Figure 1 April through June 2006 Sacramento River, San Joaquin River, Net Delta Outflow Index, and Precipitation

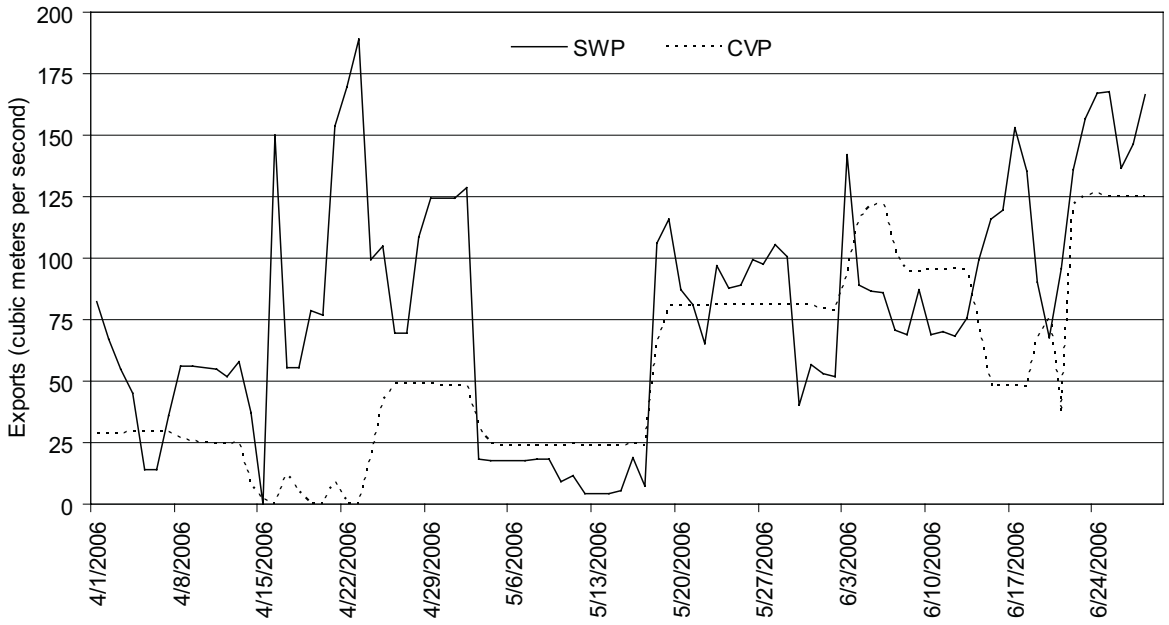

Figure 2 April through June 2006 State Water Project and Central Valley Exports

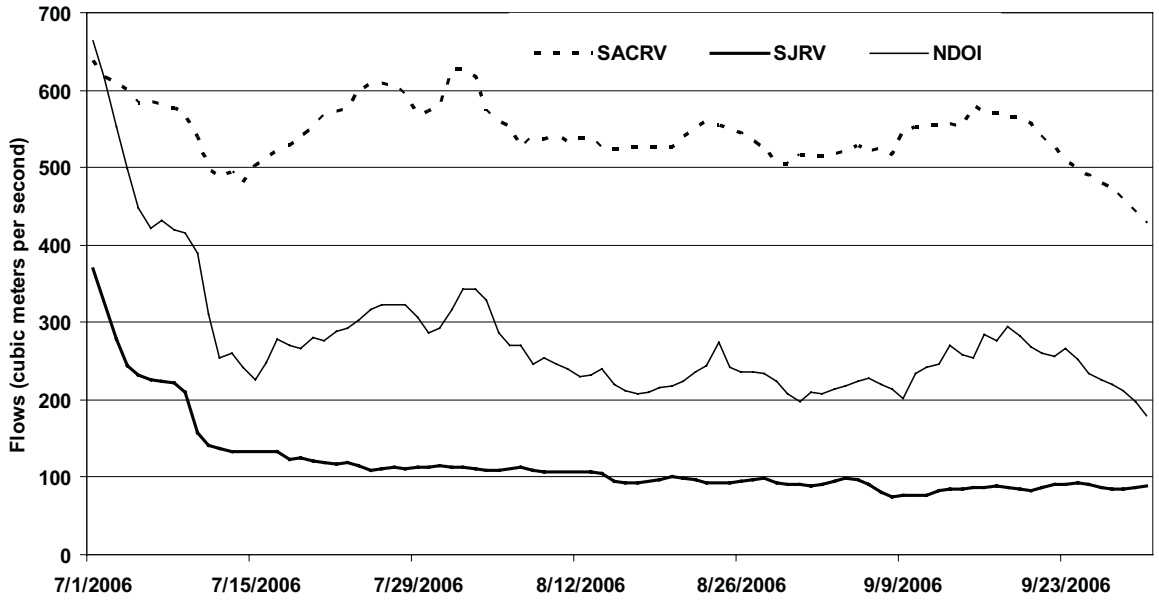

Figure 3 July through September 2006 Sacramento River, San Joaquin River, and Net Delta Outflow Index

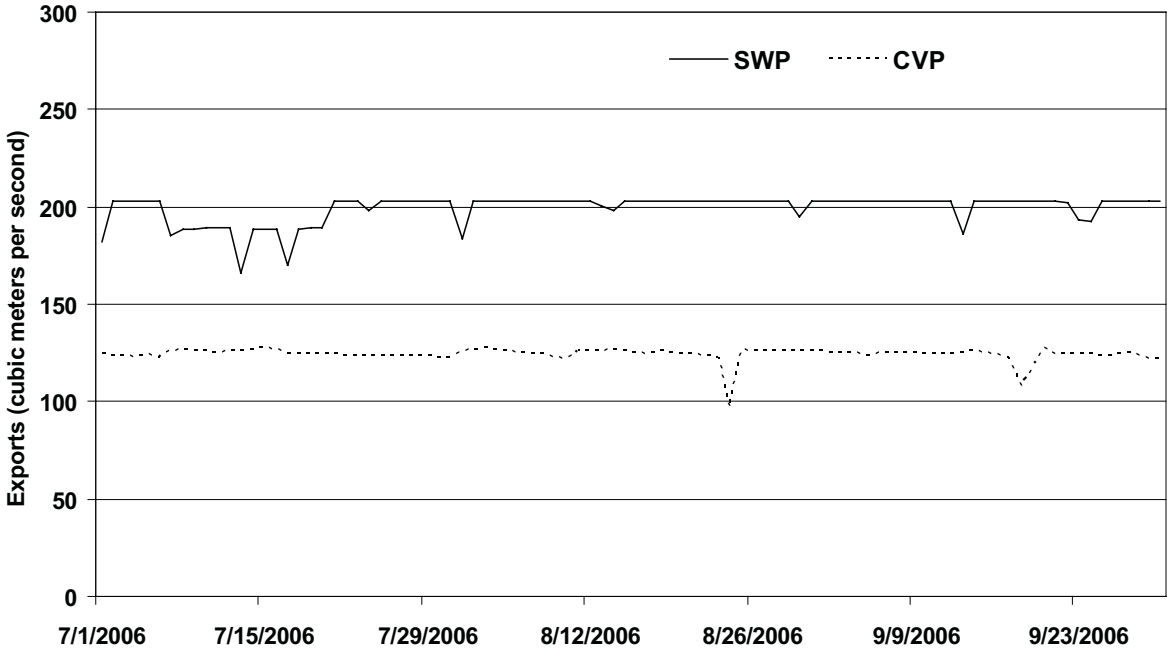

Figure 4 July through September 2006 State Water Project and Central Valley Project Exports

Fish Conservation and Culture Lab (FCCL), Fall 2006

Theresa Rettinghouse (UCD), trettinghouse@earthlink.net

Presented here is a summary for spawned captive (wild caught) delta smelt for March – May 2006. This year we used manual expression and in-vitro fertilization (strip-spawning) exclusively. We had a total of 1823 wild smelt at the lab as of March 1, and therefore an estimated 911 females during the spawning season. Fish were checked for readiness weekly and the females were separated into a single tank. Ripe females were then pulled out and strip spawned approximately once a week based on a production schedule to fill our grow-out facility. A total of 306 ripe females was used to produce a total of 385,337 delta smelt eggs. The average number of eggs per female was 1259. Healthy fertilized eggs (311,136) were then placed into our column and basket incubators. A total of 272,791 delta smelt larvae hatched 8-10 days later and were placed into larval tanks at the lab.

Percent hatch of strip-spawned eggs during 2006 (70.8%) was comparable to 2004 (75.2%) and 2005 (70.1%). Two changes were implemented this season to improve production efficiency. Bentonite (clay particles) was added to the eggs to reduce their adhesive quality and coarse sand was added to the column incubators to better fluidize the sand bed. Both of these changes helped to keep the eggs separate and suspended in the water column.

STATUS AND TRENDS

Authors reporting through 2004

Common Shrimp of the San Francisco Estuary: 2004 Status and Trends Report

Kathryn Hieb (DFG), khieb@dfg.ca.gov

Annual abundance trends from 1980-2004 and distributional patterns for 2003 and 2004 are summarized in this article for the San Francisco Estuary's most commonly collected shrimp species. The 2005 shrimp samples were not processed by April 2006, but the data should be available by late 2006. Most of the shrimp data is from the San Francisco Bay Study (Bay Study) otter trawl, with additional *Exopalaemon modestus* data from the UC Davis Suisun Marsh otter trawls and the USFWS beach seine.

The 2003 and 2004 abundance indices of juvenile *Crangon franciscorum,* the California bay shrimp, were almost identical to the 2001 and 2002 indices (Figure 1). Freshwater outflow in spring 2003 and 2004 was very similar, about double outflow in spring 2001 and 2002. The relationship between juvenile *C. franciscorum* abundance and March-May outflow remains strongly positive (both variables log transformed, $r^2 = 0.530$, n=25), with both 2003 and 2004 slightly below the fitted line. Since *C. franciscorum* is estuary-dependent and rears in shallow brackish areas, this relationship has been hypothesized to be partially due to changes in the amount of low-salinity shoal habitat, which decreases in low outflow years. Based on the total (all sizes) *C. franciscorum* index, it was again the 2nd most common shrimp species collected in the estuary in 2003 and 2004 (Table 1). However, over the entire study period *C. franciscorum* has been the most common shrimp species collected.

Distribution of *C. franciscorum* was very similar in 2003 and 2004, with shrimp collected from South Bay to the lower Sacramento River near Threemile Slough and the lower San Joaquin River to just above Antioch. In spring and summer, the highest catches were from our stations near the Dumbarton and San Mateo bridges in South Bay and from the San Pablo Bay shoals to Suisun Bay. As salinities increased over summer, the center of distribution moved slowly upstream, and by fall, the highest catches were from Suisun Bay to Honker Bay.

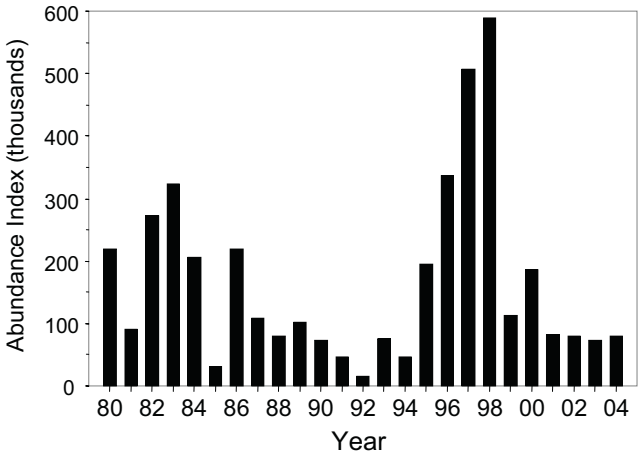

Figure 1 Annual abundance of juvenile *Crangon franciscorum*, May-October, otter trawl

The abundance of *Crangon nigricauda*, the blacktail bay shrimp, decreased in 2003 from the record high 2002 index and decreased again in 2004 (Table 1), but remained well above the study-period average. *C. nigricauda* abundance has been high since 2000 and it has been the most abundant shrimp species in the estuary since then. Although we do not understand why the *C. nigricauda* index increased to these record highs, this abundance trend was shared with the Dungeness crab and several estuarine demersal fishes, including the bay goby, staghorn sculpin, plainfin midshipman, English sole, and speckled sanddab (see the estuarine fish and crab articles in the spring newsletter). These species have varied reproductive strategies, as some spawn in the ocean and others in the estuary. All rear in polyhaline (18-30 ppt) areas of the estuary and, although common in Pacific coast estuaries, are not estuary-dependent.

C. nigricauda rears in cooler, higher salinity water than *C. franciscorum* and was collected from South Bay to Carquinez Strait in 2003 and 2004. There were 2 large year classes of *C. nigricauda* collected in 2003, late-winter adult shrimp were most common in Central Bay channels through summer and juvenile shrimp most common in San Pablo Bay from summer through fall. In 2004, adult catches were again highest at our Central Bay channel stations through summer, but juvenile shrimp were collected earlier than in 2003. Juvenile *C. nigricauda* catches were highest at several South Bay shoal stations in April and the Central Bay and lower San Pablo Bay shoal stations from May through August. There was a slow movement of juveniles to the Central Bay channel through late summer and fall as they matured.

The abundance index of *Crangon nigromaculata*, the blackspotted bay shrimp, increased slightly in 2003 and 2004 (Table 1), but both indices were below the study-period average. This species is found in cooler, higher salinity water than either *C. franciscorum* or *C. nigricauda* and is the most common species collected in the nearshore ocean area adjacent to the estuary (SFPUC 2003). In 2003 and 2004, *C. nigromaculata* was collected from South Bay to upper San Pablo Bay, with the highest catches at the channel stations just south of Yerba Buena Island and near Angel Island in Central Bay.

In 2003 and 2004, abundance of *Heptacarpus stimpsoni,* the Stimpson coastal shrimp, decreased (Table 1), following 4 years of increasing indices. This is similar to the trend observed for *C. nigricauda*. *H. stimpsoni* was collected from South Bay to upper San Pablo Bay in 2003 and 2004, with the highest catches at the 2 channel stations south of Yerba Buena Island and several channel stations in Central and lower San Pablo bays.

Abundance of *Palaemon macrodactylus*, the introduced oriental shrimp, decreased in 2003 from 2002, and then increased slightly in 2004 (Table 1). Both the 2003 and 2004 indices were below the study-period mean and it remained a minor component of our total shrimp catch. As this species prefers structured shallow water habitats, such as vegetation and pilings, it is more common in the estuary than our sampling indicates. In 2003 and 2004, *P. macrodactylus* was most common in South Bay, near the Dumbarton Bridge, and from Carquinez Strait to the channel near Pittsburg.

As in 2002, *P. macrodactylus* was uncommon at our lower Sacramento River stations in 2003 and 2004, with only 9 collected in 2003 and 27 in 2004 (0.7% and 4%, respectively, of the total *P. macrodactylus* catch upstream of San Pablo Bay). In 2001, we collected 400 *P. macrodactylus* at these same stations, which was 10.9% of the total *P. macrodactylus* catch upstream of San Pablo Bay. From 2002-2004, *Exopalaemon modestus* was the dominant shrimp species in the lower Sacramento River (see next section). Both *E. modestus* and *P. macrodactylus* rear in shallow areas with vegetation or structure, so *P. macrodactylus* abundance declines may have resulted from competitive interactions with or predation by *E. modestus.*

Table 1 Annual abundance indices (thousands) of the 5 most common shrimp species and all shrimp species combined, February-October, otter trawl. The indices include all sizes (juveniles and adults) for each species.

Year	C. franciscorum	C. nigricauda	C. nigromaculata	Heptacarpus	Palaemon	All species
1980	225.7	46.4	1.7	1.0	4.7	279.5
1981	119.2	22.1	0.5	0.5	5.1	147.4
1982	366.4	16.0	1.5	0.2	3.0	387.1
1983	328.5	38.8	16.0	0.6	1.3	385.2
1984	330.9	14.7	7.8	3.1	7.0	366.4
1985	57.8	19.7	3.1	3.1	3.9	88.3
1986	258.6	55.6	6.7	2.9	5.5	334.7
1987	142.9	75.5	9.6	6.8	2.4	238.9
1988	98.6	111.8	10.7	8.6	1.7	231.5
1989	100.2	118.6	22.1	27.4	4.6	273.1
1990	67.3	168.6	44.8	19.9	3.5	304.7
1991	51.4	190.3	63.0	41.1	4.7	350.8
1992	24.8	134.7	66.4	18.5	4.5	249.0
1993	70.5	128.1	78.6	25.4	4.0	308.3
1994	48.0	102.0	56.0	15.9	2.1	224.5
1995	180.6	78.8	33.1	4.3	3.7	302.3
1996	287.0	159.4	35.3	14.9	2.2	501.3
1997	444.5	163.9	43.4	9.1	4.9	667.9
1998	540.6	128.5	53.1	4.8	9.0	739.0
1999	159.5	134.6	42.0	13.2	4.1	354.3
2000	157.5	242.7	20.7	42.2	3.1	467.5
2001	92.9	259.6	12.0	56.6	5.2	427.0
2002	96.1	652.9	15.0	78.0	4.9	848.7
2003	77.3	379.5	15.7	67.5	1.5	544.2
2004	91.7	333.7	20.5	29.0	1.9	477.5

We first collected, *Exopalaemon modestus,* the Siberian prawn, in the lower Sacramento River in 2000 and its abundance and distribution rapidly expanded in the San Francisco Estuary and its watershed within the next 1 to 2 years. The Bay Study collected only 3 *E. modestus* in 2000 but almost 10,000 in 2002 (Table 2). Its numbers also increased rapidly in Suisun Marsh (Schroeter and Moyle 2003) and in several other locations, including Liberty Island and the Yolo Bypass (USFWS unpublished data, Zeug et al. 2002). Although abundance in the Bay Study, Suisun Marsh, and Liberty Island surveys abundance peaked in either 2002 or 2003, abundance at several upstream areas, such as Knights Landing and the San

Joaquin River upstream of Stockton, continued to increase in 2004 (Table 2).

As of 2002, *E. modestus* was the most common caridean shrimp in the lower Sacramento and San Joaquin rivers, outnumbering both the native *Crangon franciscorum* and the introduced *Palaemon macrodactylus* in these areas. A similar trend was reported for Suisun Marsh, where it was the most common caridean shrimp collected in 2002, 2003, and 2004 (Schroeter and Moyle 2003 and 2004, UC Davis unpublished data).

Coincident with this population growth, *E. modestus* spread rapidly throughout the Sacramento-San Joaquin delta to non-tidal freshwater areas upstream of the delta and brackish water areas outside of Suisun Marsh. As of late 2004, it ranged from Knights Landing (Yolo County) on the Sacramento River in the north, to Mud Slough (Merced County), a tributary of the San Joaquin River, in the south (Figure 2). It was also found throughout Suisun, Grizzly, and Honker bays to Carquinez Strait, and infrequently in San Pablo Bay.

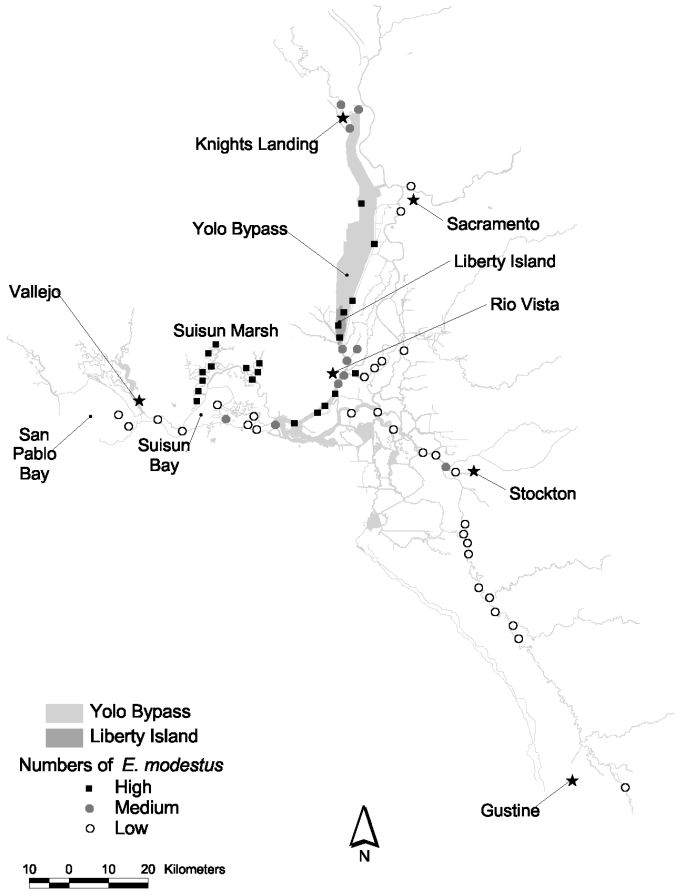

Figure 2 Distribution map for *Exopalaemon modestus*, showing areas of highest abundance, 2002-2004

Acknowledgements

I thank Ken DeVore of DFG and Tiffany Brown of DWR for production of the *Exopalaemon modestus* distribution map, Ali Stover and Robert Schroeter of UC Davis for the unpublished Suisun Marsh data, and Jonathan Speegle of USFWS for the unpublished beach seine data.

Table 2 Annual catch and CPUE of Exopalaemon modestus from several studies and gears, 2000-2004. Bay Study and Suisun Marsh otter trawl CPUE is mean catch/tow and USFWS beach seine CPUE is catch/volume*0.25. Bay Study data is from January 2000-December 2004, Suisun Marsh data is from March 2002-December 2004, USFWS Liberty Island data is from August 2002-October 2004, and other USFWS beach seine data is from July 2002-December 2004.

	CDFG, Bay Study OT		*UC Davis OT*		*USFWS seine*		
	Carquinez Strait to lower Sac and SJ rivers	*Suisun Marsh*	*Suisun Marsh*	*Liberty Island*	*Knights Landing*	*San Joaquin River, Stockton to Tuolomne River*	*Bay Study*
Year	*Catch*	*CPUE*	*Catch*	*CPUE*	*CPUE*	*CPUE*	*CPUE*
2000	3	0.01					
2001	2163	8.94					
2002	9929	41.37	7636	36.36	1.08	0.11	0.01
2003	8022	30.39	13557	53.80	0.25	0.56	0.03
2004	3696	14.11	3201	12.70	0.04	1.26	0.07

References

Schroeter, R. E. and P.B. Moyle. 2003. Trends in fish populations of Suisun Marsh, January 2002-December 2002. Annual Report for: Contract SAP 4600001965, California Department of Water Resources, Central Division, Sacramento, California. Department of Wildlife, Fish and Conservation Biology, UC Davis, 69 pp.

Schroeter, R. E. and P.B. Moyle. 2004. Trends in fish populations of Suisun Marsh, January 2003-December 2003. Annual Report for: Contract SAP 4600001965, California Department of Water Resources, Central Division, Sacramento, California. Department of Wildlife, Fish and Conservation Biology, UC Davis, 45 pp.

SFPUC. 2003. Southwest Ocean Outfall Regional Monitoring Program, Five-Year Summary Report, 1997-2001. San Francisco Public Utilities Commission, Water Quality Bureau, Environmental Services Division, San Francisco, California.

Zeug, S., G. O'Leary, T. Sommer, B. Harrell, and F. Feyrer. 2002. Introduced palaemonid shrimp invades the Yolo Bypass. IEP Newsletter 15(1):13-15.

Fish Salvage at the State Water Project and Central Valley Project Fish Facilities in 2004.

Russ Gartz(DFG), rgartz@dfg.ca.gov

Author is reporting outside the reporting period for this newsletter thus closing the gap for this data.

Introduction

The Tracy Fish Collection Facility (TFCF, Federal Facility) and the Skinner Delta Fish Protective Facility (SDFPF, State Facility) divert (salvage) fish from water exported from the upper San Francisco Estuary. The TFCF began operation in 1957 and the SDFPF began operation in 1968. Both the TFCF and the SDFPF use a louver-bypass system to salvage fish from the exported water. The salvaged fish are returned to the upper San Francisco Estuary by loading the salvaged fish into tanker trucks and trucking them to predetermined release sites.

Exports

The SWP exported roughly 3.96 billion m^3 (3,214,000 acre-feet or AF) of water in 2004 less than the 4.37 billion m^3 (3,546,000 AF) exported in 2003. Water exports ranged from a low of 56 million m^3 (45,023 AF) in May to a high of 524 million m^3 (424,810 AF) in January. Monthly exports were lowest from April through June and highest from January through March and June through July (Figure 1). Exports increased from October through December (Figure 1).

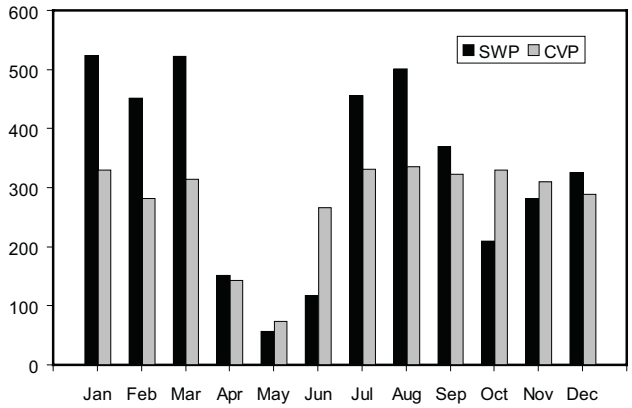

Figure 1 Monthly water exports (million m3) for the SWP and CVP, 2004

The CVP exported roughly 3.32 billion m^3 (2,695,000 AF) of water in 2004 less than the 3.43 billion m^3 (2,784,000 AF) in 2003. Water exports ranged from a low of 73 million m^3 (58,984 AF) in May to a high of 336 million m^3 (272,383 AF) in August. With the exception of April through June, monthly exports ranged from 281 – 366 million m^3 (215,762 – 272,383 AF) (Figure 1).

Fish Salvage

The composition of salvage at both facilities was dominated by threadfin shad, striped bass, and American shad in 2004. At SWP, roughly 1.84 million fish (34 species) and mitten crabs were salvaged. At CVP, roughly 5.87 million fish (45 species) and mitten crabs were salvaged. At SWP, threadfin shad accounted for 63% of the annual salvage, followed by striped bass and American shad (Figure 2). These 3 species constituted 91% of the annual salvage. At CVP, threadfin shad accounted for 73% of the annual salvage followed by striped bass and American shad (Figure 3). These 3 species constituted 90% of the annual salvage. Generally speaking, the proportion of annual salvage represented by threadfin shad

has been increasing since 1989 (Figure 4). Density of fish (individuals salvaged per 10,000 m^3) was highest at SWP in July through August, while at CVP it was highest from November through December (Figure 5).

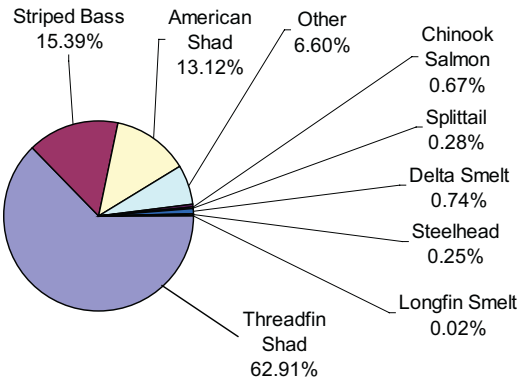

Figure 2 Percentage of annual salvage of the most prevalent species and species of concern at the SWP, 2004

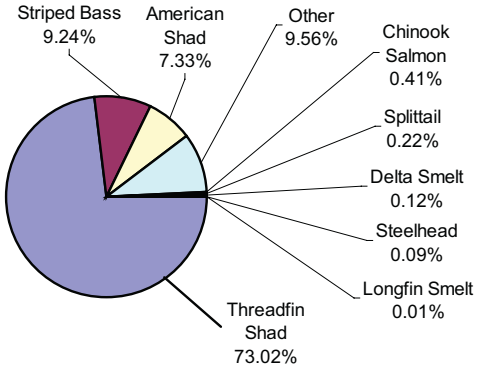

Figure 3. Percentage of annual salvage of the most prevalent species and species of concern at the CVP, 2004

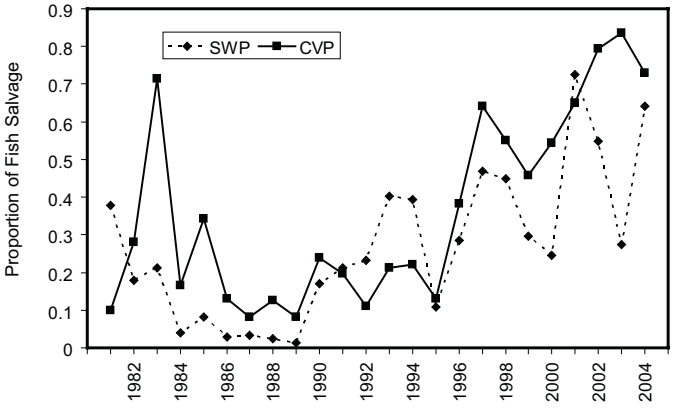

Figure 4 Relative proportion of threadfin shad in annual salvage at the SWP and CVP, 1981 - 2004

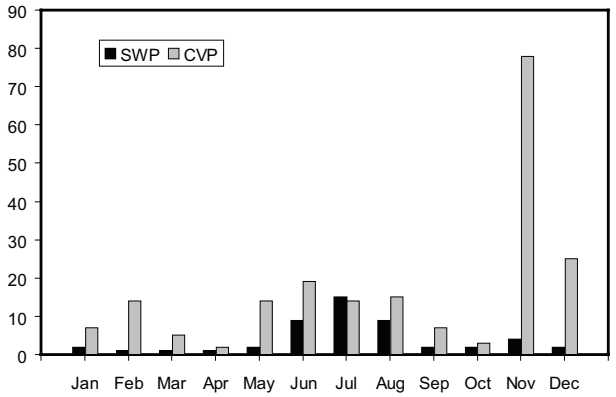

Figure 5 Monthly density (ind/10,000 m3) of fish salvaged at th SWP and CVP, 2004

Delta Smelt

The annual salvages of delta smelt continued a declining trend since 2002 at both facilities (Figure 6). At SWP, 13,694 delta smelt were salvaged in 2004 as opposed to 21,248 in 2003. At CVP, 6,769 delta smelt were salvaged in 2004 as opposed to 16,662 in 2003. Prior to 1988, the salvage of delta smelt was higher at CVP (except for 1983 and 1986) and from 1988 and onwards the salvage of delta smelt is higher at SWP (except for 1998) (Figure 6). Delta smelt salvage in 2004 occurred primarily in 2 pulses: January through March and May through June (Figure 7).

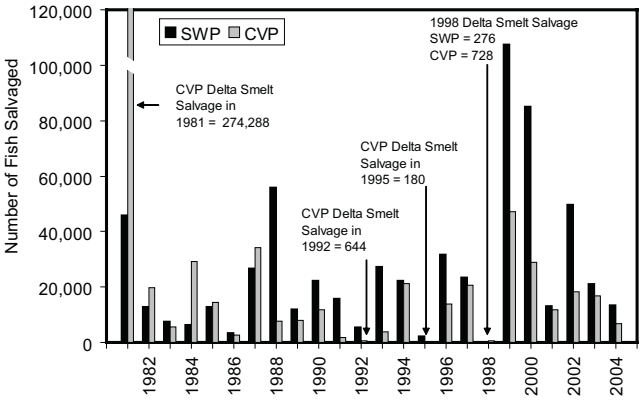

Figure 6 Annual salvage of delta smelt at the SWP and the CVP, 1981 - 2004. The salvage at CVP in 1981 has been truncated for scale considerations

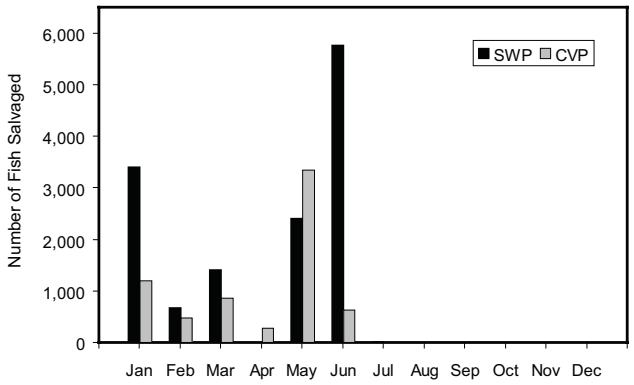

Figure 7 Monthly salvage of delta smelt at the SWP and the CVP, 2004

Chinook Salmon

The combined salvages of Chinook salmon (wild, hatchery, and unknown origin[1]) were low in 2004; continuing the trend of low salvage since 2001 (Figure 8). At SWP, combined salvage was 12,411 in 2004 as opposed to 17,492 in 2003. At CVP, combine salvage was 24,217 in 2004 as opposed to 16,498 in 2003.

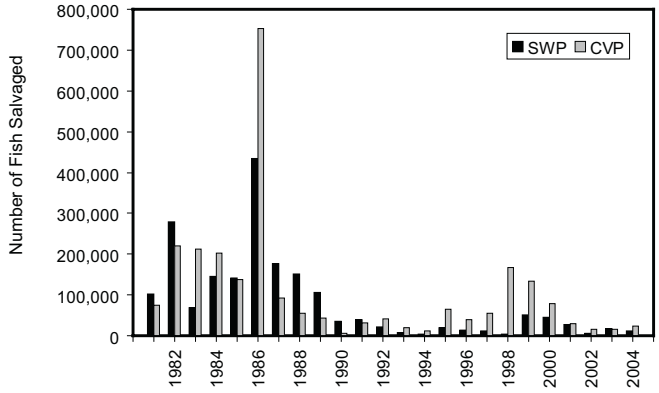

Figure 8 Annual salvage of Chinook salmon (wild and hatchery combined) for the SWP and the CVP, 1981 - 2004

The annual salvages and losses of Chinook salmon in 2004 were composed of primarily wild fish. The salvage of fish of unknown origin was 102 for both facilities combined, less than 1% of the overall salvage. Salvage was higher at CVP while loss (an estimate of mortality resulting from entrainment) was higher at SWP. Combining both facilities, 29,161 wild fish (7,728 at SWP and 21,433 at CVP) were salvaged as opposed to 7,365 hatchery fish (4,665 at SWP, 2,700 at CVP). Combining both facilities, 46,715 wild fish were lost (33,381 at SWP and 13,334 at CVP). The loss of hatchery fish was 20,186 at SWP and 1,806 at CVP for a combined loss of 21,992.

The salvage and loss of wild fish was primarily composed of fall and spring-run and to some extent, winter-run sized fish (Table 1). Race is determined by length alone for salvage/loss considerations. Fall run wild fish contributed to 51% of the wild fish salvage at SWP and 84% at CVP. Fall-run wild fish contributed to 51% of the loss of wild fish lost at SWP and 83% of the wild fish lost at CVP. Salvage/loss of wild Chinook salmon occurred primarily from February through May (Figure 9). Of particular note, the salvage of 15,720 in March at CVP accounted for 73% of all wild Chinook salmon salvage at CVP (Figure 9).

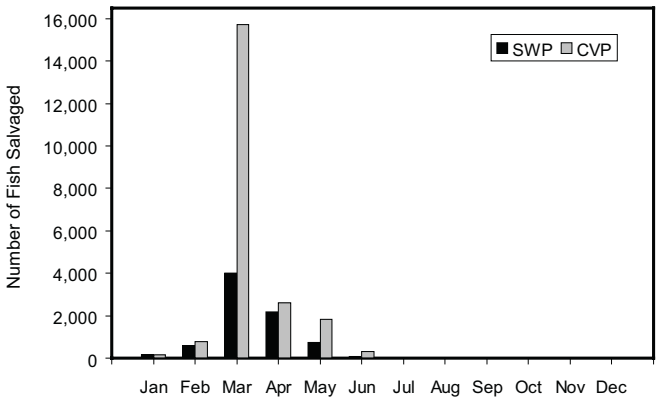

Figure 9 Monthly salvage of wild Chinook salmon at SWP and the CVP, 2004

1. Chinook salmon of unknown origin are fish that were counted, but no adipose clip status was recorded.

Table 1 Wild salmon salvage and loss by race for the SWP and the CVP, 2004

Race	SWP Annual Salvage	CVP Annual Salvage	Total Salvage	SWP Annual Loss	CVP Annual Loss	Total Loss
Fall	3,922	17,976	21,898	16,859	11,066	27,925
Late-fall	18	37	55	80	24	104
Spring	2,188	2,352	4,540	9,458	1,532	10,990
Winter	1,600	1,068	2,668	6,984	712	7,696
Total	7,728	21,433	29,161	33,381	13,334	46,715

Steelhead

The combined salvages of steelhead in 2004 were less than 2003. The SWP salvaged 4,605 steelhead in 2004 as opposed to 5,766 in 2003. The CVP salvaged 5,186 steelhead in 2004 as opposed to 6,871 in 2003. However, salvages in 2003 and 2004 are much larger than in 2002 (Figure 10), and the all time low salvages of 113 in 1998 at SWP and 14 in 1983 at CVP.

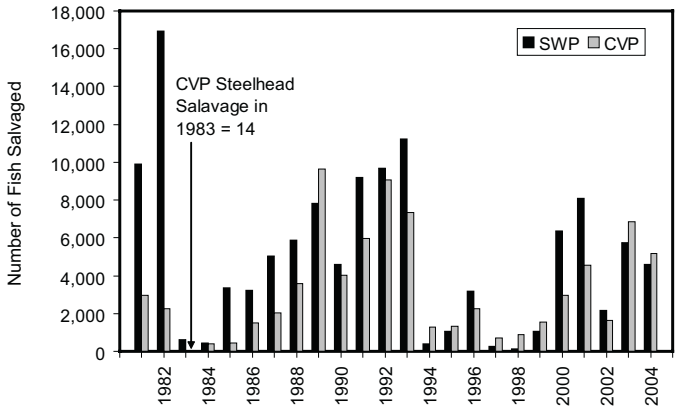

Figure 10 Annual salvage of steelhead (wild and hatchery combined) for the SWP and the CVP, 1981 - 2004

The salvage of steelhead in 2004 was predominately hatchery fish. The SWP salvaged 3,622 hatchery steelhead, comprising 79% of the annual salvage. The CVP salvaged 4,354 hatchery steelhead, comprising 84% of the annual salvage. The SWP salvaged 983 wild steelhead while the CVP salvaged 832 occurring predominately from January through May (Figure 11).

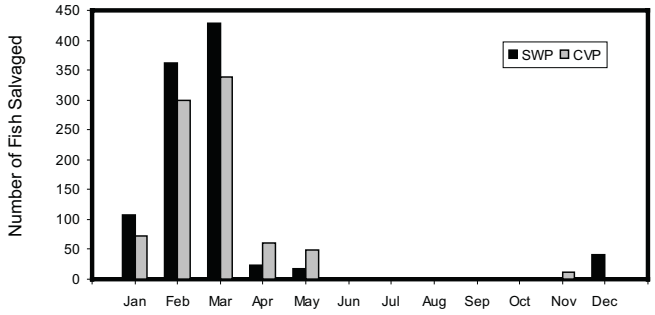

Figure 11 Monthly salvage of wild steelhead for the SWP and the CVP, 2004

Striped Bass

The salvages of striped bass at both facilities were low in 2004, a trend that started in 1994 and has been broken only in 2000 at SWP (Figure 12). Salvage at SWP was 284,006, roughly 1/3 of the salvage in 2003 (753,549). Salvage at CVP was 542,072, over 3 times that in 2003 (165,358). However, even these salvages are proportionally small when compared to previous salvages, especially before 1989, when annual salvages were commonly in the millions (Figure 12).

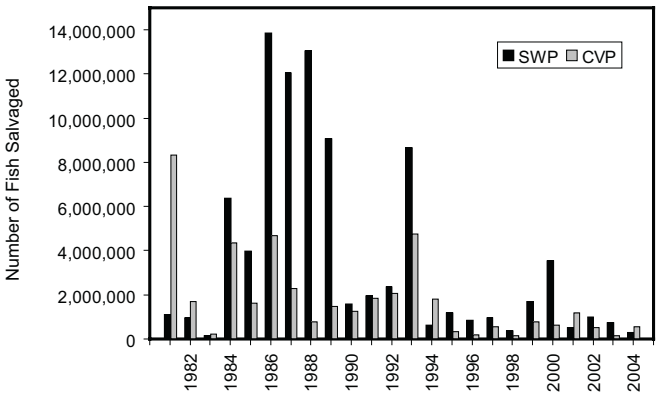

Figure 12 Annual salvage of striped bass at the SWP and the CVP, 1981 - 2004

Salvage of striped bass occurred in all months in 2004 at both facilities (Figure 13). Salvage at SWP ranged from 2,635 in April to 76,284 in June. Salvage at CVP ranged from 2,811 in October to 279,240 in June. The June monthly salvage at CVP accounted for 52% of the annual salvage.

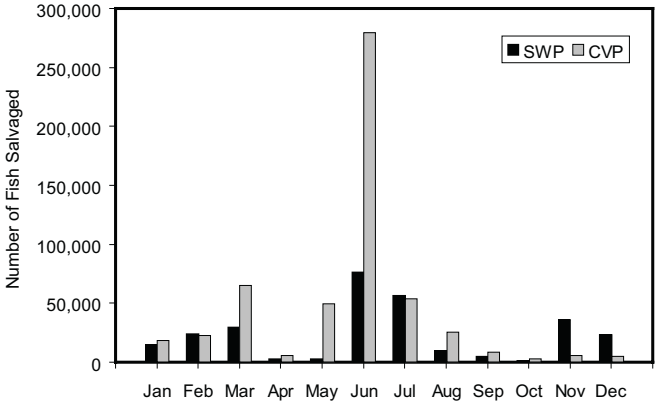

Figure 13 Monthly salvage of striped bass at the SWP and the CVP, 2004

American Shad

The salvages of American shad at both facilities were less in 2004 than in 2003; more so at SWP. The salvage at SWP in 2004 was 242,780, roughly 12% of the salvage in 2003 (2,023,039). The salvage at CVP was 429,978, roughly 88% of the salvage in 2003 (488,033). The majority of annual salvages of American shad at either facility are less than 1,000,000 with the exceptions of 1995, 1996, 2000, and 2003 at SWP (Figure 14).

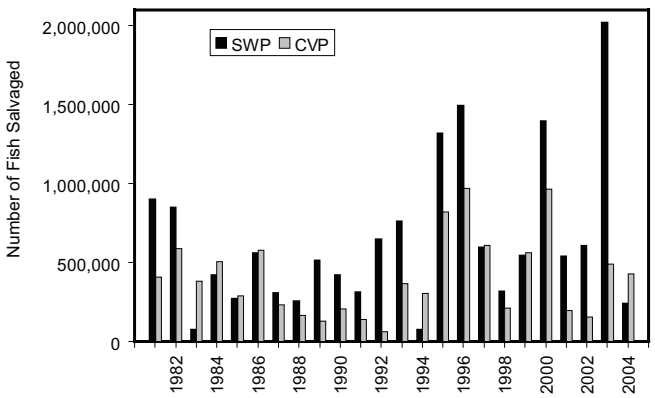

Figure 14 Annual salvage of American shad at the SWP and the CVP, 1981 - 2004

Salvage of American shad occurred during all months for both facilities. At SWP, salvage ranged from 157 in May, to 82,979 in July (Figure 15). At CVP, salvage ranged from 348 in May to 282,012 in November (Figure 15). The July salvage at SWP accounted for 34% of the annual salvage while the November salvage at CVP accounted for 66% of the annual salvage.

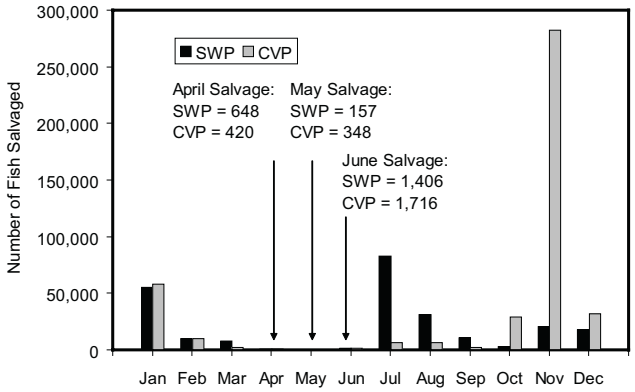

Figure 15 Monthly salvage of American shad at the SWP and the CVP, 2004

Splittail

The salvages of splittailwere low at both facilities in 2004, but not unusually low. The SWP salvaged 5,176 and the CVP 13,131. Both salvages were somewhat less than the salvage in 2003: 6,066 at SWP and 13,666 at CVP. The lowest salvages for the period of record, 1981 – 2004, both occurred in 1994: 277 at SWP and 2,824 at CVP. Large salvages of splittail (for this species, greater than 150,000) have occurred only in 1982, 1983 (CVP only), 1986, 1995, and 1998 (Figure 16). Salvage of splittail in 2004 occurred predominately in February and

March at the SWP and in May and June at the CVP (Figure 17).

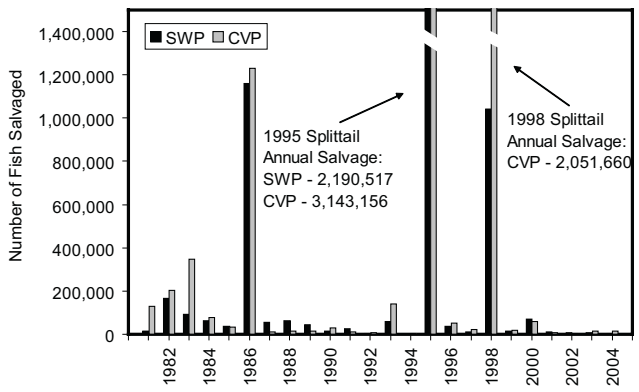

Figure 16 Annual salvage of splittail at the SWP and the CVP, 1981 - 2004

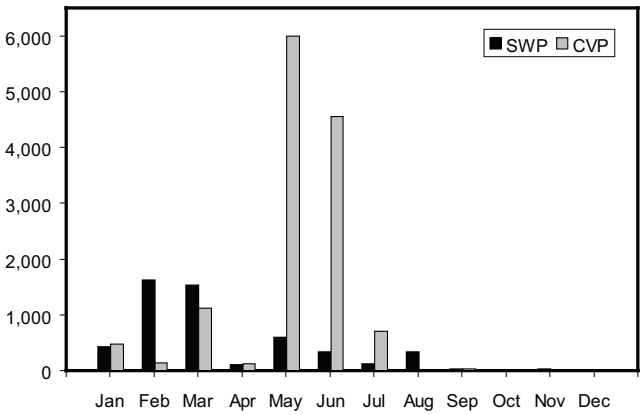

Figure 17 Monthly salvage of splittail at the SWP and the CVP, 2004

Longfin Smelt

Although the salvages of longfin smelt at both facilities were low in 2004, they were not all-time lows or unusual. The salvage at SWP was 333 and at CVP was 648; both lower than salvages in 2003 (SWP: 706, CVP: 4,562). However, the lowest salvages for the period of record, 1981 - 2004, are: SWP, 52 in 1982; and CVP, 0 in 1995. The low salvages in 2004 were not unusual in that since 1990, salvage of longfin smelt has been low, with the exception of 2002 (Figure 18). Large salvages (over 10,000) have occurred only once since 1990 (Figure 18). Salvage of longfin smelt in 2004 occurred primarily in January at the SWP and in April-May at the CVP (Figure 19).

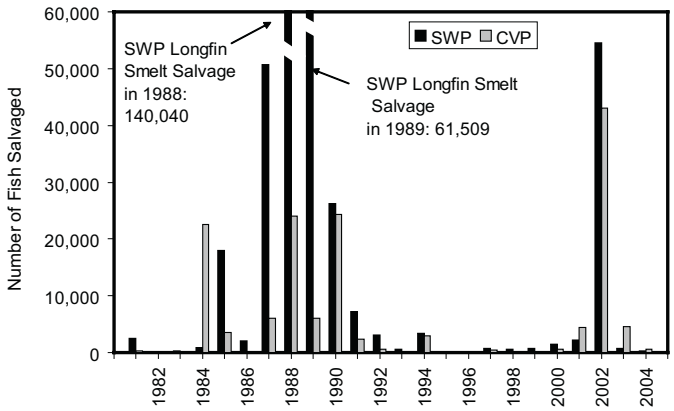

Figure 18 Annual salvage of longfin smelt at the SWP and the CVP, 1981 - 2004

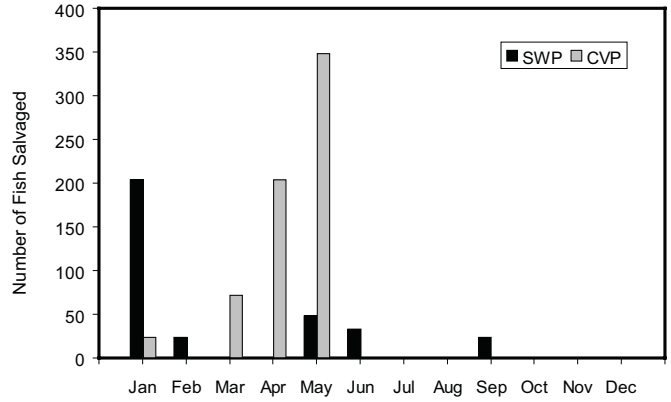

Figure 19 Monthly salvage of longfin smelt at the SWP and CVP, 2004

Chinese Mitten Crabs

The salvage of Chinese mitten crabs (mitten crabs) was low for both facilities in 2004. In general, mitten crabs have been in decline since 2001 for both facilities (Figure 20). The salvage of mitten crabs at SWP was 366. This is an increase from 2003 (160) but much lower than the highest annual salvage from the period of record (1999 – 2004) of 33,903 in 1999. The salvage of mitten crabs at the CVP was 745, a new low for the period from 1999 – 2004. This is slightly less than the salvage in 2003 (804) and much less the high for the period of record, 25,104 in 1999. Salvage of mitten crabs occurred primarily in October at the SWP (72% of annual salvage) and at the CVP (71% of annual salvage).

Figure 20 Annual salvage of mitten crabs at the SWP and the CVP, 1999 - 2004

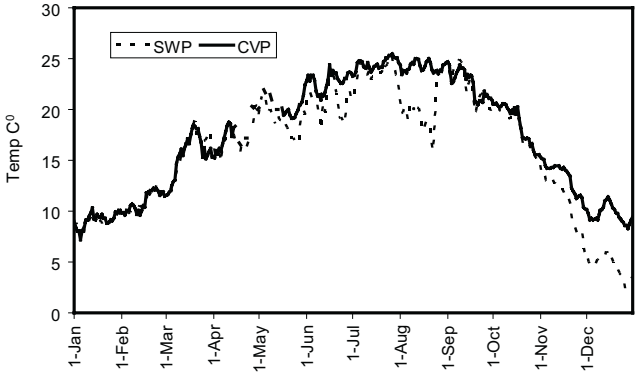

Figure 21 Mean daily temperature (degrees C0) for the SWP and the CVP, 2004

Temperature

Daily mean temperature at both facilities showed the expected annual pattern: low at the beginning of the year, peaking in summer (late July), and a declining trend thereafter (Figure 21), with indications that there were periods when the temperatures were cooler at SWP than CVP. The most noticeable cool periods are from July 28th to August 25th and November 4th to December 31st (Figure 21). However, given the close proximity of the 2 facilities, the "cool" periods at SWP (Figure 21) are questionable and may be the result of a faulty temperature sensor at SWP. A similar problem was documented by Foss (2003) at the SWP in 2002. Given the above, I will report the temperature range and mean annual temperature for the CVP only: 7 to 25 C^0 with a mean of 17 C^0.

Salvage data can be obtained from DFG's Central Valley Bay-Delta Branch Web Site - http://www.delta.dfg.ca.gov/Data/Salvage/

References

Foss S. 2003. Fish salvage at the State Water Project and Central Valley Project Fish Facilities. Interagency Ecological Program Newsletter, Volume 16, Number 2, pages 40-45.

CONTRIBUTED PAPERS

Estimating Dissolved Inorganic Carbon Concentrations from Salinity in San Francisco Bay for Use in ^{14}C – Primary Production Studies

A.E. Parker(SFSU),aeparker@sfsu.edu, J. Fuller, R.C. Dugdale

Introduction

One of the most fundamental measurements used for characterizing marine environments is primary production, the production of organic matter from inorganic constituents (most commonly through photosynthesis). Primary production estimates are typically made using the radioactive carbon -14 tracer technique introduced by Steeman Nielsen (1952) where the investigator adds a trace amount of radioactive carbon to a water sample and quantifies the radioactive enrichment of particulate organic matter during an incubation period. The technique is dependent upon precise determination of both radioactive enrichment and ambient dissolved inorganic carbon (DIC) concentration in the sample. While determining radioactivity is relatively easy with the use of a liquid scintillation counter, direct determination of DIC concentrations is often more difficult as few laboratories have the necessary instrumentation available. Traditionally in oceanic studies, DIC concentrations were based on a constant approximate value of 2000 µmol L^{-1} (i.e. Eppley & Sharp, 1975; Sharp, personal communication, see "Notes") or based on measurements of salinity and pH (Parsons et al., 1984). These methods of approximation can be made within a salinity range of 22 – 33 psu (Parsons et al., 1984) and are therefore of limited use for work in estuaries, such as the San Francisco estuary (SFE), where salinity varies between 0 and >33 psu. Previous ^{14}C based estimates of primary production in the SFE required direct determination of DIC concentrations (e.g. Cole & Cloern, 1984, Jassby et. al.2002).

Spiker & Schemel (1979) measured alkalinity in the SFE from locations beginning at the confluence of the Sacramento and San Joaquin Rivers to the Golden Gate and found that total alkalinity followed a simple linear relationship (i.e. conservative behavior) with salinity in the northern estuary suggesting that alkalinity is sufficiently invariant over the time scale of estuarine mixing. Cifuentes et. al., (1990) showed some non-linearity due to variations in river discharge and endmember concentrations in the SFE, but the deviation from a conservative mixing model was slight. Assuming that total alkalinity is approximately equal to carbonate alkalinity and that *in situ* processes that affect DIC in the estuary (i.e. photosynthesis and respiration) are small relative to the total DIC pool, DIC should also behave conservatively in the SFE. Alkalinity and DIC have been shown to behave conservatively in other estuaries such as the Delaware (Sharp et al., 1982) where an empirically derived relationship between DIC concentration and salinity has been determined from >300 DIC – salinity pairs (Sharp, et al., in prep). Due to differences in DIC concentration between the DIC sources of various estuaries, it is unlikely that a DIC – salinity relationship developed for one estuary could be applied successfully to all others (Cai & Wang, 1998). For example, differences between DIC concentrations in the Atlantic and Pacific are, in part, responsible for different DIC - salinity relationships for the Delaware and San Francisco estuaries. The goal of this study was to investigate the relationship between DIC and salinity for the San Francisco estuary and to develop an equation that could be used to estimate DIC concentrations from salinity for use in SFE productivity studies.

Methods and Materials

Samples for salinity and DIC were collected during cruises aboard the RV Polaris along full SFE transects beginning in South San Francisco Bay USGS "Sta 36" at Calaveras Pt. (38º 28.3'N, 122º03.9'W) and ending in the northern estuary at USGS Sta "657" at Rio Vista (38º08.9'N, 121º41.3'W). Maps of the USGS monthly transects have been published previously (e.g. Cloern, 1987). Sampling was conducted during four research cruises (July 2005, August 2005, February 2006, and April 2006) in which a total of 183 DIC - salinity pairs were obtained. We sampled from the ship's flow-through

system which pumps near surface bay water (ca. 2m depth) from an inlet on the bow of the ship. Salinity measurements were recorded in the flow through system using a Sea-bird SBE 19 SeaCat conductivity sensor. The instrumentation package is calibrated annually by the manufacturer with periodic comparisons made by the USGS using a second CTD package to evaluate accuracy (Schraga, personal communication, see "Notes"). Time and ship position were logged concurrently with temperature and salinity every 2 seconds. River distance was calculated by summing the best fit lines between collection points using Rio Vista to the north as 0 km; USGS "Sta. 36" in the South Bay is 141 km "down river" from Rio Vista.

The samples for DIC measurement were collected from the ship's flow-through system downstream of the conductivity sensor. In order to match DIC and salinity values, we noted the time that DIC collection began and ended and averaged the salinity over the period of collection (ca. 30 seconds). Glass scintillation vials (25 ml) were filled and allowed to overflow for a volume equal to several times vial volume taking care to exclude bubbles. Samples were preserved with 200 µl of 5% w/v $HgCl_2$ and sealed with an inverted poly-cone cap which displaced water ensuring no headspace in the sample vial. Samples were then stored at 4ºC in the dark for up to 24-hr before DIC analysis was completed.

DIC was measured on an acid-sparging - nondispersive infrared analyzer (NDIR) system originally developed at the Monterey Bay Research Institute (Walz & Friedrich, 1996; Parker, 2005). The system works by injecting a 1.25 ml sample into an acid-sparging column with 300 µl 5% H_3PO_4 acid. Carbon dioxide is stripped out of solution by bubbling with oxygen carrier gas and passed through a $Mg(ClO_4)_2$ drying column then measured with a LICOR-6252 integrating NDIR infrared CO_2 analyzer. The instrument was standardized using Scripps certified reference material (prepared in the laboratory of A. Dickson). Three replicate injections were run for each sample to yield replicate precision (expressed as coefficient of variation, CV) of 0.07% (ca. ± 1.5 µM) for standards and 0.42% CV for estuarine samples.

Results and Discussion

The spatial distribution of dissolved inorganic carbon in the San Francisco estuary can be generalized by results from the transect completed in April 2006 (Fig 1). Using distance from the Golden Gate (km), DIC concentrations were relatively constant from 100 - 58 km with an average value of 1057 ± 63 µM. During the four surveys DIC concentrations in the freshwater region (<1 psu) of the estuary varied between 976 µM – 1216 µM; the highest average DIC for the freshwater region during a single transect was in August 2005 when the average was 1203 µM. Freshwater DIC values are remarkably similar, despite seasonal differences in freshwater supply to the estuary. River flow ranged between 269 - >5500 m^3 sec^{-1} for the four transects (Dayflow; http://www.iep.ca.gov/dayflow/).

Dissolved inorganic carbon concentrations and salinity increased along the transect from Rio Vista (Figure 1). The positive relationship between salinity and DIC continued into Central San Francisco Bay (ca. -15 km) where we observed the highest salinities during each transect. This is not surprising as Central Bay has a direct connection to the Pacific Ocean via the Golden Gate. Beyond Central San Francisco Bay salinity decreased with decreasing river distance while DIC concentration continued to increase. The highest DIC was found consistently at the most southern point surveyed in South San Francisco Bay.

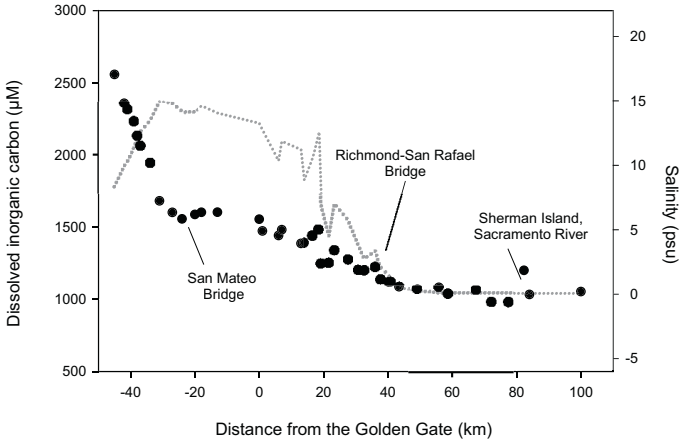

Figure 1 Dissolved inorganic carbon concentrations (closed circles) along a sampling transect from Rio Vista to south of the Dumbarton Bridge in the San Francisco estuary in April 2006. Salinity (grey line) was measured continuously using an underway flow-through system along the transect

South San Francisco Bay is characterized by low freshwater input and relatively long residence times (Clo-

ern & Oremland, 1983). South Bay receives its main freshwater supply from the sewage outfalls of the City of San Jose (Hager & Schemel, 1996). Spiker & Schemel (1979) suggested that the major source of DIC to South San Francisco Bay was from sewage effluent and noted high alkalinity in this region of the estuary. The relatively long residence time of South San Francisco Bay may also lead to higher DIC concentrations from the respiration of accumulated organic matter. In addition, the salt ponds of the South San Francisco Bay may provide an additional source of DIC as carbonate salts leach into the South San Francisco Bay basin.

By plotting DIC concentrations against salinity, 2 distinct mixing lines that result from 3 DIC sources to the bay become readily apparent (Figure 2). For each of the sampling dates, DIC concentrations appear to behave quasi-conservatively in the estuary from 0 psu to the high salinity Central Bay for each sampling date, This suggests that for the northern and Central estuary, DIC is a function of dilution between the riverine DIC source and the Pacific Ocean DIC source. For points moving into South San Francisco Bay, DIC concentrations exhibited an inverse relationship with salinity. The South Bay mixing lines produce "fingers" as a result of variability in source water DIC concentrations (Figure 2). DIC concentrations at USGS Sta. 36, south of the Dumbarton Bridge, during the four surveys ranged from 2300 to 3009 µM. We cannot explain the high degree of variability in source water DIC in the South Bay but it may be due to changes in sewage effluent discharge or seasonal changes in freshwater discharge to the South Bay diluting the DIC supply from effluent sources. As a result of the variability there, it does not appear that a simple salinity - DIC relationship exists for the South San Francisco Bay though the distribution of DIC appears to be a function of dilution between the sewage DIC source and the Pacific Ocean.

By isolating the data that fall within the range of salinities between the freshwater endmember and Central San Francisco Bay, the relationship between salinity and DIC concentration can be approximated by a linear function (Figure 3, Table 1). Linear least-squares regressions were fit to the data from each of the four transects. The resulting slopes varied between 28.3 and 35.2 with intercept values between 1056 and 1199. The range in DIC concentrations in the freshwater endmember from July 2005, August 2005 and April 2006 was between 977 and 1186 (Table 1). The lowest DIC concentration measured in February 2006 was 1265 µM but that was from a salinity of 2.7 psu, and therefore did not represent the freshwater endmember. The range of highest DIC concentrations collected on each cruise reflects the highest salinity values that were observed in Central San Francisco Bay (Table 1). From these data, it appears that the freshwater source of DIC to the SFE is consistent over the annual cycle. The least-squares regression of pooled data ($r^2 = 0.98$, $p < 0.0001$, $n = 113$) provides an approximation of DIC for the northern and Central SFE using the equation:

$$\text{DIC } (\mu M) = 31.5 \times \text{Salinity (psu)} + 1098 \qquad (1)$$

The predicted mean square error from the regression is ±48 µM DIC. We compared these results with DIC concentrations measured by the USGS within the salinity gradient of the northern estuary (Cloern, unpublished data, see "Additional References").The USGS results also appear quasi-conservative, though the correlation between DIC and salinity is not as strong ($r = 0.84$, $n = 23$). DIC concentrations derived from equation (1) were consistently 27% higher than the measured values in the USGS. There is no way to determine whether the offset is due to methodological differences in DIC analysis between the two datasets, or an overall change in the distribution of DIC in the estuary.

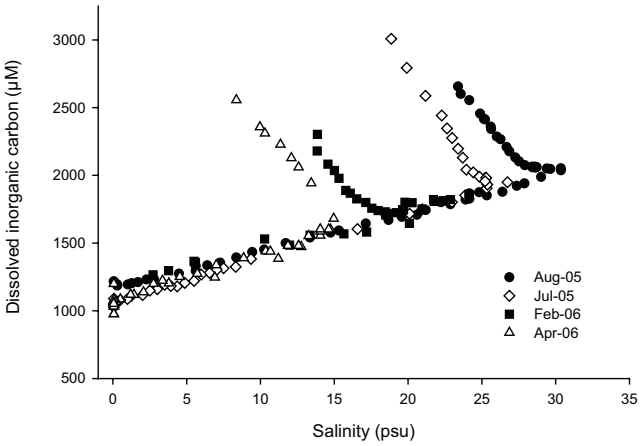

Figure 2 Dissolved inorganic carbon versus salinity along transects sampled in August 2005 (closed circles), July 2005 (open diamonds), February 2006 (closed squares) and April 2006 (open triangles)

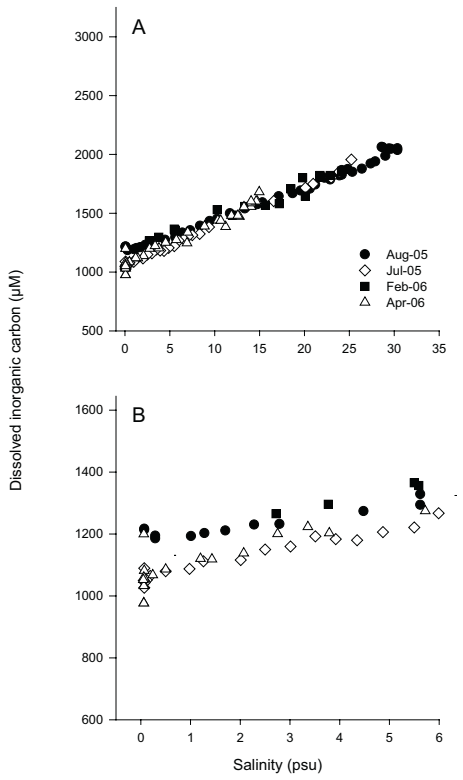

Figure 3 (A) Dissolved inorganic carbon versus salinity for the northern and Central San Francisco Estuary. Dates and legend for transects are the same as for Figure 2. Results of linear least squares regression: DIC (µM) = 31.5 x Salinity (psu) +1098 (r2 = 0.98, n = 113). (B) Dissolved inorganic carbon versus salinity for salinities between 0 and 6 (psu). Linear least squares regression: DIC (µM) = 37.5 x Salinity (psu) + 1084 (r2 = 0.63, n = 52).

To better constrain the influence of the variability in freshwater DIC concentration, we pooled DIC – salinity pairs between 0 and 6 (psu) salinity and performed a least squares regression (Figure 3B). The relationship between DIC concentration and salinity is not as strong when examined within only the low salinity range ($r^2 = 0.63$, n = 52). We calculated DIC concentrations based on salinity using equation 1 from mid salinity and low salinity points, and compared those estimates with measured DIC concentrations (Table 2). For both mid and low salinity points, the error in calculated DIC concentrations ranged between <1 and >5%. Based on the intercept of equation 1, predicted DIC concentrations in the freshwater region of the estuary are 1098 µM. We examined the USGS dataset of measured the DIC values from the Delta. Results from 6 of 9 stations sampled on 5 occasions between May and November 1997 showed that DIC concentrations ranged from 782 to 1094 µM (mean 1060 µM); this value is remarkably similar to the model prediction from equation 1. Of the 3 stations that deviated significantly from the mean, both high (2356 ±187 µM) and low (280 ± 10 µM) DIC concentration were observed. The USGS dataset illustrates the potential for localized variability in DIC concentrations in the Delta and as a result we would caution against assuming constant DIC concentrations within the freshwater region of the estuary.

Table 1 Linear least squares regression of dissolved inorganic carbon versus salinity for Central and northern San Francisco Bay. Slope, intercept and correlation coefficient, r^2, from each transect. Results of least squares regression from pooled data (all cruises) are in bold.

	Lowest DIC (µM)	*Highest DIC (µM)*	*Highest salinity (psu)*	*Regression Slope*	*Regression Intercept*	*r^2*	*n*
July '05	1027	1950	26.7	33.06	1056	*1*	*28*
Aug '05	1186	2051	30.4	28.31	1165	*0.99*	*42*
Feb '06	1265[a]	1858	24.1	26.68	1199	*0.94*	*15*
April '06	977	1681	15.0	35.20	1062	*0.94*	*28*
Pooled data				31.54	1098	*0.98*	*113*

[a] Sampling did not extend into freshwater region of the estuary

Table 2 Calculated DIC concentrations at mid and low salinity locations within the northern and Central SFE. DIC was calculated according to equation (1). Calculated DIC was compared with actual DIC concentration expressed as percent error ((Predicted DIC - Measured DIC)/ (Predicted DIC + Measured DIC)/2)) x 100%. Negative values of percent error indicate that calculated DIC < measured DIC.

Salinity	*Calculated DIC (µM)*	*Measured DIC (µM)*	*Percent Error*
20.1	1731	1717	0.8
19.8	1721	1802	-4.6
19.6	1715	1692	1.3
14.1	1542	1603	-3.9
3.8	1220	1266	-3.7
1.3	1142	1203	-5.2
1.0	1133	1088	4.0
0.5	1118	1086	2.9

Calculated DIC concentrations were compared to a weekly time series of measured DIC concentrations in Central San Francisco Bay in 2006 provided by CICORE (Center for Integrative Coastal Observations, Research and Education) program's SFBeams monitoring program (http://sfbeams.sfsu.edu/) (Figure 4). Calculated and measured DIC concentrations track each other throughout the time series with an average error of ±3% (median error ±5%). The greatest discrepancy was ca. 10%. Unlike the previously reported results obtained along the transects, salinity data used for the CICORE time series were collected from a bucket sample and measured using a handheld salinity probe (YSI Model) which may explain some of the additional error.

Although there are few reported estimates of precision for ^{14}C primary production, the original published methods reported error of ca. 15 - 30% (Steeman Nielsen, 1952; 1975). Undoubtedly precision of ^{14}C tracer methods has increased as improvements in scintillation counters have been made; more recent estimates of ^{14}C precision are ca. 8-10% (Parker, 2004). Still the error that we report here based on the difference in estimated and measured DIC concentrations (1 – 5%) are well within the experimental error associated with the ^{14}C – primary production technique. Therefore, we suggest that, for primary production studies within northern and Central San Francisco Bay, DIC may be reasonably approximated from salinity measurements. Within the low salinity region of the estuary (0 – 5 psu) calculated DIC (using equation 1) may underestimate actual concentrations.

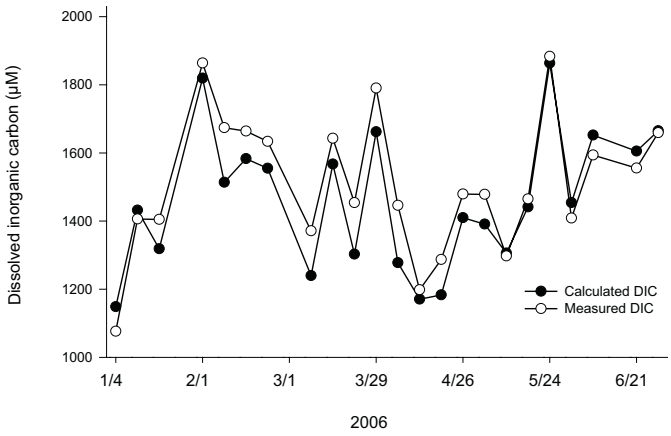

Figure 4 Time series of weekly DIC concentrations (closed circles) from Central San Francisco Bay. Calculated DIC concentrations, based on equation (1) (open circles) are also plotted. Average and median percent error were -3% and -5%, respectively.

Acknowledgements

We would like to thank James Cloern and the crew of the RV Polaris for ship support and Amy Kleckner for sample collection. Anne Slaughter and Kevin Lew supplied CICORE SFBeams data. We would also like to thank J. Cloern, J.H. Sharp, W. Kimmerer, and F. Wilkerson for comments on this manuscript.

References

Cai, W.-J. and Y. Wang (1998). The chemistry, fluxes, and sources of carbon dioxide in the estuarine waters of the Satilla and Altamaha Rivers, Georgia. Limnology and Oceanography, **43**(4): 657-668.

Cifuentes, L. A., L. E. Schemel, et al. (1990). Qualitative and numerical analyses of the effects of river inflow variations in mixing diagrams in estuaries. Estuarine, Coastal, and Shelf Science 30: 411-427.

Cloern, J. E. (1979). Phytoplankton ecology of the San Francisco bay system: the status of our current understanding. San Francisco Bay: The Urbanized Estuary. T. J. Conomos. San Francisco, Pacific Division, American Association for the Advancement of Science: 247-264.

Cloern, J. E. (1987). Turbidity as a control on phytoplankton biomass and productivity in estuaries. Continental Shelf Research 7: 1367-1381.

Cloern, J. and R. Oremland (1983). Chemistry and microbiology of a sewage spill in south San Francisco Bay. Estuaries 6: 399-406.

Cole, B. E. and J. E. Cloern (1984). Significance of biomass and light availability to phytoplankton productivity in San Francisco Bay. Marine Ecology Progress Series **17**: 15-24.

Eppley, R. W. and J. H. Sharp (1975). Photosynthetic measurements in the central North Pacific: the dark loss of carbon in 24-hr incubations. Limnology and Oceanography. 20: 981-987.

Hager, S. and L. Schemel (1996). Dissolved inorganic nitrogen, phosphorus and silicon in South San Francisco Bay I. Major factors affecting distributions. San Francisco Bay: the ecosystem. J. T. Hollibaugh. San Francisco, Pacific Division, AAAS.

Jassby, A. D., J. E. Cloern, et al. (2002). Annual primary production: Patterns and mechanisms of change in a nutrient-rich tidal ecosystem. Limnology and Oceanography 47(3): 698-712.

Parker, A. E. (2004). Assessing the phytoplankton-heterotrophic link in the eutrophic Delaware Estuary. Graduate College of Marine Studies. Lewes, University of Delaware: 277.

Parker, A. E. (2005). Differential supply of autochthonous organic carbon and nitrogen to the microbial loop of the Delaware Estuary. Estuaries 28(6): 856-867.

Parsons, D. C., Y. Maita, et al. (1984). A Manual of Chemical and Biological Methods for Seawater Analysis. Oxford, Pergamon Press.

Sharp, J.H., Yoshiyama, K., Parker, A.E., Schwartz, M.C., Curles, S.E. Beauregard, A.Y., Ossolinski, J., Davis, A., (2006) " The Chemistry of the Delaware Estuary: Seasonal and Spatial trends and correlations. Estuaries and Coasts, In review.

Sharp, J. H., C. H. Culberson, and Church, T. (1982). The chemistry of the Delaware Estuary: General Considerations. Limnology and Oceanography 27: 1015-1028.

Spiker, E. C. and L. E. Schemel (1979). Distribution and stable-isotope composition of carbon in San Francisco Bay. San Francisco Bay: the Urbanized Estuary. T. J. Conomos. San Francisco, Pacific Division, American Association for the Advancement of Science: 195-212.

Steemann Nielsen, E. (1952). The use of radioactive carbon (C14) for measuring organic carbon production in the sea. J. Cons Perm Int Explor Mer 18: 117-140.

Steemann Nielsen, E. (1975). Marine Photosynthesis with Special Emphasis on the Ecological Applications. New York, Elsevier Scientific Publishing Company.

Walz, P. M. and G. E. Friederich (1996). Rapid automated analysis of total dissolved inorganic carbon and its application in the central California upwelling system during the CoOP95 experiment. EOS 76: OS102.

Notes

Schraga, Tara. US Geological Survey, Menlo Park, CA telephone, July 25 ,2006

Sharp, Jonathan H. Professor, College of Marine and Earth Studies, University of Delaware. email, August 21, 2006

Additional References

Cloern, James. Research Scientist, U.S. Geological Survey, Menlo Park, CA. email, September 18, 2006.

The Vertical Structure of Dissipation in Tidally-Forced Shallow Water Body with Locally Generated Waves

Nicole Jones (Stanford University), nicolej@stanford.edu

Abstract

Measurements of the vertical distribution of the dissipation of turbulent kinetic energy were made, with an array of four acoustic Doppler velocimeters, in the shallow embayment of Grizzly Bay, San Francisco Bay, CA. Due to the combination of wind and tidal forcing in the shallow water body, the surface and bottom boundary layers overlap. Under conditions of whitecapping waves, dissipation of turbulent kinetic energy in the upper portion of the water column was found to be greatly enhanced, relative to the predictions of wind stress wall-layer theory. Instead, the dissipation follows a modified deep-water breaking-wave scaling. Close to the bed the dissipation measurements scaled with the bed stress log-law scaling.

Introduction

The shallow water regions of San Francisco Bay are of central ecological importance because they support net production of phytoplankton (Cloern 1996). However, benthic grazing, by siphonate bivalves, and reduced light availability, due to resuspension of sediment, can limit the growth of phytoplankton in shallow waters (Alpine and Cloern 1992; Cohen et al. 1984; Dame et al. 1980; Nichols 1985; Thompson 1999; Wildish and Kristmanson 1984). Phytoplankton is an important food source for upper trophic levels. Consequently animal populations, such as fish, may suffer under conditions of high benthic bivalve grazing (Feyrer and Healey 2003). Despite recognition of the importance of shallow water habitat to the greater Bay/Delta region, there is a limited understanding of the flow structure, mixing, light variability and benthic grazing in these regions.

Tide-driven pressure gradients and surface wind stresses provide the dominant forcing of the shallow waters of San Francisco Bay. These forces determine both the bottom friction and the vertical mixing, which in turn dictate the distribution of phytoplankton. For example, increased bottom stress due to wind-waves resuspends larger amounts of sediment thereby reducing the level of irradiance to which the phytoplankton populations are exposed. If the vertical mixing time scale is shorter than the phytoplankton production time scale, a surface bloom is unlikely because the phytoplankton will be mixed over the water column depth in a much shorter time than it can be produced in the euphotic zone, thereby enhancing the losses to aphotic zone respiration and benthic grazing. Understanding vertical mixing and bottom stress as a function of the hydrodynamic conditions is essential to be accurately model these regions.

Shallow (<3 m) embayments in estuaries often experience wind waves that alter the bottom friction and vertical mixing, thereby influencing the distribution of constituents such as phytoplankton in the water column. Studies of the surface layer of oceans and deep lakes have shown that wave breaking and rotational waves lead to increased levels of turbulence in the upper portion of the water column. In shallow water, where the bottom boundary layer, due to tidal forcing, may overlap with this surface layer. The resulting wave-current interactions are not well understood.

At the water surface, momentum is transferred from the wind to the water column. A surface wind stress will create a wall layer extending from the air-water interface downward, analogous to the bottom boundary layer. However, the wind momentum also creates surface waves which in turn transfer momentum to the surface current field by enhancing turbulent kinetic energy (TKE) near the surface via processes such as wave breaking.

Surface waves have the potential to modify the dynamics near the free surface in three ways (Craig and Banner 1994). The most well understood mechanism is Stokes drift, a Lagrangian current in the direction of the waves, resulting from the unclosed orbits of wave motion. The second influence of waves is the generation of a Reynolds stress on the mean motion due to waves that are not perfectly irrotational. The third mechanism is the result of breaking waves generating TKE that is available to be mixed down into the surface layer. The influence of the enhanced turbulence is to reduce mean velocities below those anticipated for log-layer behavior. Laboratory and field measurements have shown that there is a region of enhanced turbulence to a depth of approximately k^{-1}, where k is the wavenumber, below which "law of the wall" behavior exists (Agrawal et al. 1992; Anis and Moum 1995; Drennan et al. 1996; Kitaigorodskii 2001; Kitaigorodskii and Lumley 1983; Soloviev and Lukas 2003; Terray et al. 1996). The third mechanism will be the focus of this study.

A central parameter used to describe and model turbulence dynamics is the rate of TKE dissipation, i.e., the rate at which turbulence produced (typically) by shear at large scales is transferred to smaller scales and ultimately converted to heat (Tennekes and Lumley 1972). Measured dissipation rates are known to be elevated under waves and to decay with depth to a power between 2 and 4 (Kitaigorodskii 1983; Terray et al. 1996). Drennan et al. (1996) found that dissipation was 1 to 2 orders of magnitude larger than wall layer theory predicts. Terray et al. (1996) scaled data collected in a large, deep lake with the wave height and wind energy input to the waves and found that dissipation decayed with depth to a power of -2. More fully developed ocean waves have also been found to follow this relationship (Drennan et al. 1996).

Craig and Banner (1994) employed a numerical model with the Mellor-Yamada level 2.5 turbulence closure model to predict near surface dissipation under breaking wave conditions. The breaking waves were incorporated into the model as a source of turbulent kinetic energy at the surface. Model results predict a dis-

sipation decay of $z^{-3.4}$ in the wave-enhanced layer, well within the range of the observations. Furthermore, the model illustrates that there is a balance between the dissipation and the downward flux of TKE from the surface, in this layer. Below this, the flow follows the classic law of the wall behavior where shear generation is balanced by dissipation (Craig and Banner 1994).

In shallow water, it is likely that the bottom and surface layers will overlap, thereby altering the theoretical profiles. Bricker (2005) found that under wave-dominated regimes the constant stress layer did not extend far from the bed. The excess shear stress was attributed to the shear stress generated at the free surface. Recent measurements of dissipation of TKE in a nearshore region with white-capping waves, by Feddersen et al. (2007), have shown that in the surface layer the deep-water breaking wave scaling of Terray et al. (1996) applies. However, at this location the negligible vertical shear in the mean currents leads to values of shear production that are much smaller than dissipation at all depths. In a tidally forced environment, the bottom boundary layer would be expected to be strongly sheared and therefore shear production of turbulence is expected to be an important source of turbulence close to the bed. The purpose of this study is to quantify the effect of whitecapping on the distribution of turbulence in a shallow water body where the surface wind/wave driven boundary layer and bottom tidally forced boundary layers overlap.

Field measurements

The measurements were collected in Grizzly Bay, San Francisco Bay, California (Figure 1), from 1st May-2nd June 2005. An array of four acoustic Doppler velocimeters (Nortek, Vector) recorded velocity and pressure, at four heights above the bed (0.15 m, 0.5 m, 1.5 m and 2 m) in a water column of mean depth 2.5 m (Figure 2), synchronized with a capacitance wave-height gauge (RBR, WG50). The pressure gauges and capacitance wave gauge were sampled for a period of 10 minutes at 16 Hz every 30 minutes. A chain of five thermistors (Seabird) and two conductivity sensors were used to identify any periods of stratification. Vertical profiles, with 10 cm spatial resolution, of the mean velocity were measured with a Doppler current profiler (Nortek, Aquadopp Profiler). A wind anemometer (R. M. Young Company), situated approximately 6 m above mean water level, nearby on D7 (Figure 1 Experimental layout and Figure 3), recorded wind velocity statistics every 10 minutes. A record of "sea state" was gained via a high resolution camera which recorded 5 images every hour (Figure 3).

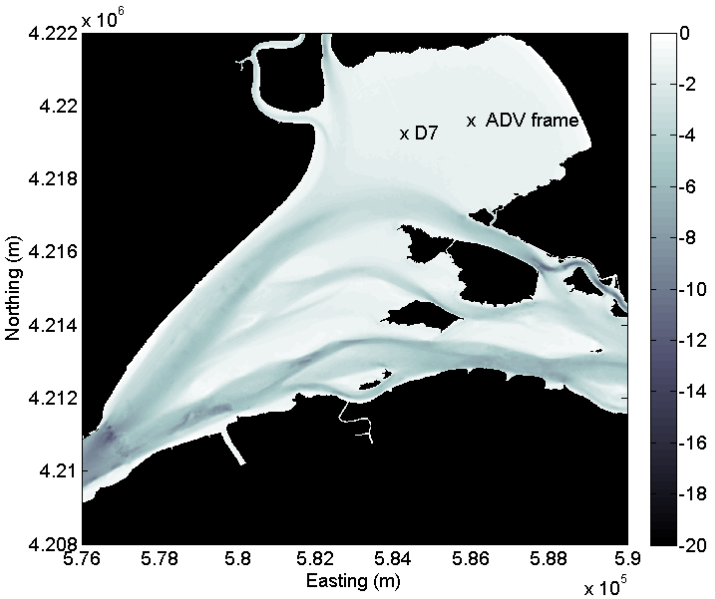

Figure 1 Experimental layout. Bathymetry in meters

Figure 2 ADV frame

Figure 3 Wind anemometer and camera located at D7

The instruments were located approximately in the center of the embayment, which has a mean depth of approximately 2.5 m and a mean tidal range of 1.8 m. Depth averaged maximum currents at the measurement location were approximately -0.15 m/s on ebb and 0.25 m/s on flood. Wind stress was derived from the measured wind velocity via the Donelan (1990) algorithm which was developed for fetch limited lakes and accounts for the effect of waves and whitecapping on the wind stress. The estimated wind stress in the primary direction of the current ranged from 0 to 0.4 m^2s^{-2} with a median value of 0.06 m^2s^{-2}. The waves that are present are locally generated with a mean period varying between 1.2 and 1.4 s and root mean square wave heights ranging from 0 to 0.5 m. Due to the bathymetry of the embayment, which acts to refract the waves towards the shoreline, the wave direction is predominantly 45 ^{o} (Figure 4).

The dominant current direction was identified using principal component analysis and the three components of the ADV velocities were transformed into this coordinate system, u (positive flood tide) and w (positive upward).

The dissipation of TKE was calculated from the ADV data. Each ADV vertical velocity 10 minute record was divided into 31 sections of equal length, each with 50% overlap. Each segment was windowed with a Hanning window and the fast Fourier transform calculated. All 63 spectral estimates were ensemble averaged to produce a resultant spectral estimate with 126 degrees of freedom. The expected spectral value is within 0.82 and 1.25 of the sample value at 90 % confidence limits.

Dissipation was calculated from a -5/3 fit to the inertial sub-range of the vertical velocity spectra, beyond the wave peak, employing the Lumley and Terray (1983) model to account for the effects of waves on the turbulent wave number spectrum (Feddersen et al. 2007; Trowbridge and Elgar 2001). The bed stress is calculated via the Shaw and Trowbridge (2001) method, which decomposes the wave and turbulent stresses.

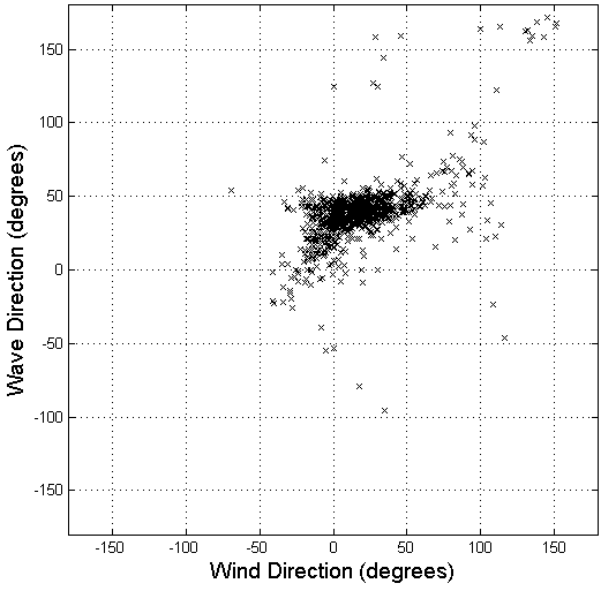

Figure 4 The wave direction remains predominantly 45 ^{o} over wind directions from -25 o to 50 ^{o} due to wave refraction within the embayment

Results

The typical vertical structures of dissipation under condition of weak winds (< 4m/s) and strong winds (8-10 m/s) are shown in Figure 5 a and b respectively. In these figures, the depth is normalized to take into account variation in water column height due to the tide and the magnitude of the depth averaged velocity is distinguished by the color of the data point. Under weak wind conditions, where wave heights are very small, the magnitude of the dissipation is approximately equal for a particular current magnitude in the bottom half of the water column (Figure 5a). The values of dissipation increase with large current magnitudes as expected. The larger levels of dissipation

close to the water surface are due to night-time convective cooling. Typical night time conditions during the experiment lead to a rate of buoyant production of TKE on the order of 10^{-7} m^2s^{-3}. Under stronger wind speeds, a pattern consistent with the weak wind speeds is seen only in the bottom 10% of the water column (Figure 5b). The upper 90% of the water column contain dissipation values significantly higher than those at the bed. Closest to the surface,dissipation is up to three orders of magnitude larger than near-bed values.

If the influence of breaking waves on turbulence is insignificant, then the magnitude of the dissipation should be explained by classic boundary layer theory which assumes production and dissipation are in balance. The assumption that production and dissipation are in balance leads to the following scaling for dissipation for the bottom boundary layer:

$$\varepsilon = \frac{u_{*b}^3}{\kappa z} \tag{1}$$

where u_{*b} is the bed stress, $K=0.41$ is the Karman constant, and z is the height above the bed; and dissipation for the wind-driven surface boundary layer:

$$\varepsilon = \frac{u_{*w}^3}{\kappa z'} \tag{2}$$

where u_{*w} is the stress due to the wind and z' is the depth below the surface. The depth is scaled with u_{*b}^2/g and u_{*w}^2/g for the bottom boundary layer and wind-driven surface boundary layer respectively.

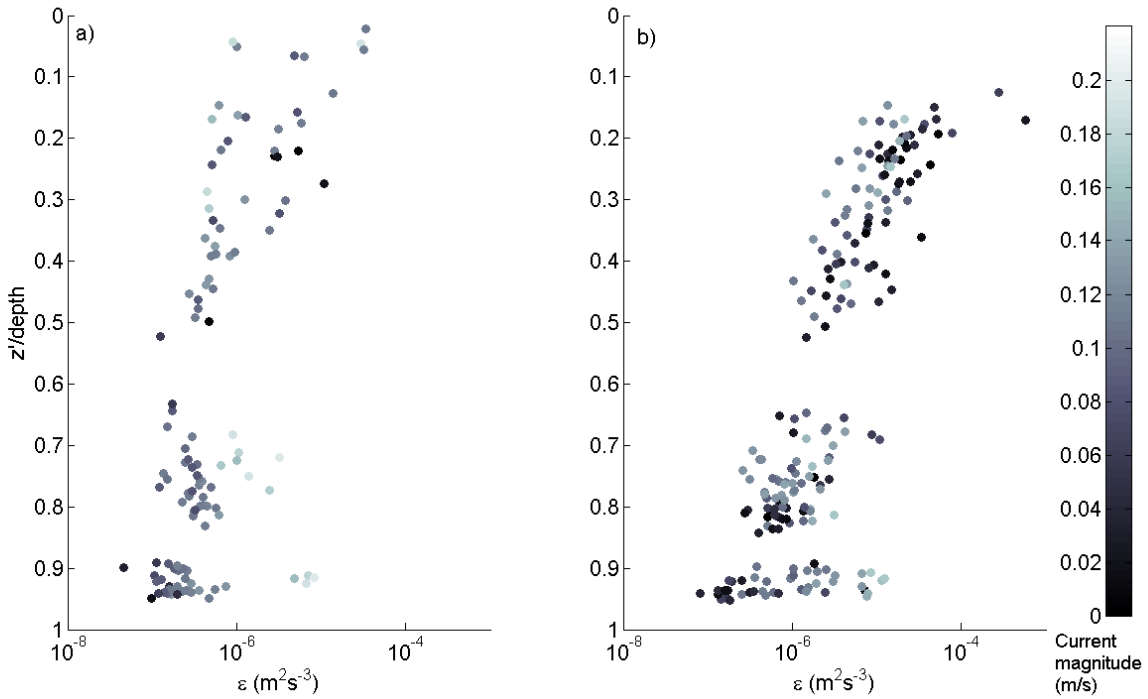

Figure 5 Vertical profiles of the dissipation of TKE over the normalized depth. Profiles are shown for conditions of a) weak wind velocity (0-4 m/s) and b) strong wind velocity (8- 10 m/s). The magnitude of the depth averaged velocity is distinguished by the color of the data point.

If it is assumed that ADV1 (0.15 m above the bed) was within the constant stress layer, the bed stress can be estimated using the Shaw and Trowbridge (2001) decomposition method. Figure 6 illustrates that, very close to the bed, wall-scaling applies, however, the measurements deviate higher in the water column as the wind stress begins to influence the rate of dissipation.

The ADVs near the surface measured an enhanced dissipation rate of TKE close to the air-water interface, when waves are present, relative to the predictions of wall-layer theory (Figure 7). The large range of non-dimensional dissipation values for each non-dimensional depth is due to the range of wave conditions experienced for each wind stress. The growth of the waves and hence the extent of whitecapping is a function of the longevity of the wind stress. Below the surface enhanced layer, the dissipation values are close to the wall-layer values, agreeing with previous studies (Agrawal et al. 1992) . At greater depths the dissipation of TKE begins to be dominated by the presence of the bed and deviates again from the wind-driven surface boundary layer theory. The transition between the surface layer and bottom layer varies with wind and tidal forcing conditions and therefore is not defined in Figure 7.

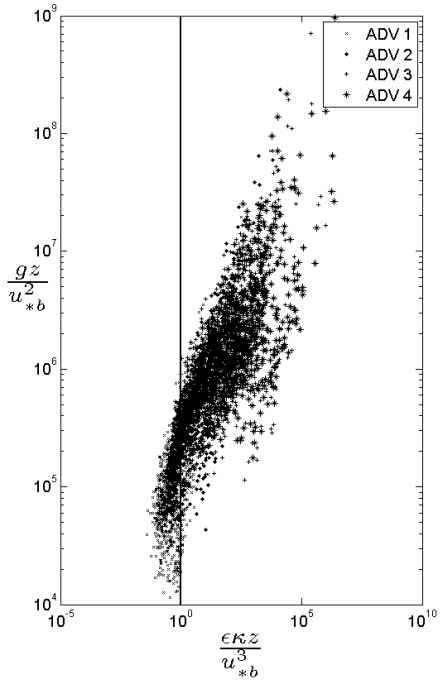

Figure 6 Dissipation normalized using wall-layer scaling, turbulent production via bed stress. The vertical line is the prediction of wall-layer theory.

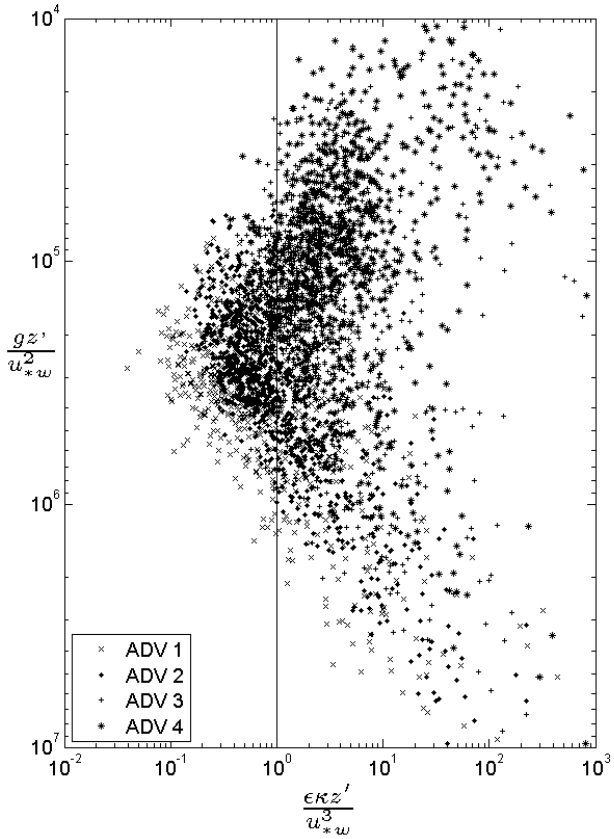

Figure 7 Dissipation normalized using wall-layer scaling, turbulent production via wind stress. The vertical line is the prediction of wall-layer theory

Terray et al. (1996) developed an alternative scaling of dissipation to account for the observations of enhanced dissipation in the surface layer. The scaling is based on the assumption that wave breaking is the principal source of TKE in the near surface layer and that breaking directly injects energy to depth z_b' . The energy in this "breaking layer" is then transported downward and simultaneously dissipated. Dissipation is normalized by F/H_s where F is the rate of energy input to the waves from the wind and H_s is the significant wave height. The depth below the surface, z' , is normalized by the significant wave height H_s. Terray et al. (1996), and a number of studies that followed (e.g. Drennan et al. 1996), found that their data could be described by

$$\frac{\varepsilon H_s}{F} = 0.3\left(\frac{z'}{H_s}\right)^{-2} \qquad z_b < z' < z_t \tag{3}$$

where $z_b' \approx 0.6H_s$ and $z_t' \approx 3.6H_s\overline{c}/u_{*a}$ are the length scales of the breaking zone and transition depth to wall layer respectively, where $\overline{c}$ is the effective phase speed, defined as

$$F \equiv \frac{\tau_a \overline{c}}{\rho_w} \approx u_{*w}^2 \overline{c} \tag{4}$$

Following, Terray et al. (1996) the rate of energy input to the waves from the wind *F*, is defined as

$$F = g\int \frac{\partial S_\eta}{\partial t} d\omega d\theta = g\int \beta S_\eta d\omega d\theta \tag{5}$$

where $S_\eta(\omega,\theta)$ is the directional spectrum of the waves and β is the e-folding scale for the temporal growth of wave energy in the absence of nonlinear interactions and dissipation. The formulation for β used in this study, developed by Donelan and Pierson (1987) is

$$\frac{\beta}{\omega} = 0.194\frac{\rho_a}{\rho_w}\left(\frac{U_{\pi/k}\cos\phi}{c(k)} - 1\right)\left|\frac{U_{\pi/k}\cos\phi}{c(k)} - 1\right| \tag{6}$$

where for a wave component of wave number *k*, having phase speed *c*, the magnitude *U* and direction ϕ of the wind are evaluated at a reference height of π/k.

The Terray et al. (1996) relationship (Eq. (3)) approximates the data reasonably well in terms of the slope, however, a lower non-dimensionalized dissipation is generally found for a particular non-dimensionalized depth. This may be due to errors in the estimation of the rate of energy input to the waves from the wind *F* (Eq. (5)) which requires the use of a formulation for the integral growth rate over the wave spectrum (Eq. (5)). The formulation for β (Eq. (6)) is not a definitive relationship and can be site and condition specific. At depth the data deviate, presumably due to the influence of the bed stress due to the tidal pressure gradient. The transition depth z_t' proposed by Terray et al.(1996), does not match the data well for the same reason. In fact, in the presence waves, a wall stress log-layer region is probably uncommon. Instead the bottom tidal boundary layer most likely transitions directly to the wave enhanced surface layer.

The numerical model of Craig and Banner (1994) predicted the dissipation decay rate as:

$$\frac{\varepsilon z_0}{\alpha u_{*w}^3} = 2.4\left(1 + \frac{z'}{z_0}\right)^{-3.4} \tag{7}$$

where αu_{*w}^3 is defined to be the kinetic energy flux at the surface. Terray et al. (1996) proposed that if $z_0 \sim H_s$ and $\alpha \sim F/u_{*w}^3$ then the relationships agree in the asymptotic limit of Eq. (7). Using the lengthscale and kinetic energy flux at the surface in Eq. (7) proposed by Terray et al. (1996), the data from the two ADVs closest to the surface agrees well with the model (Figure 8).

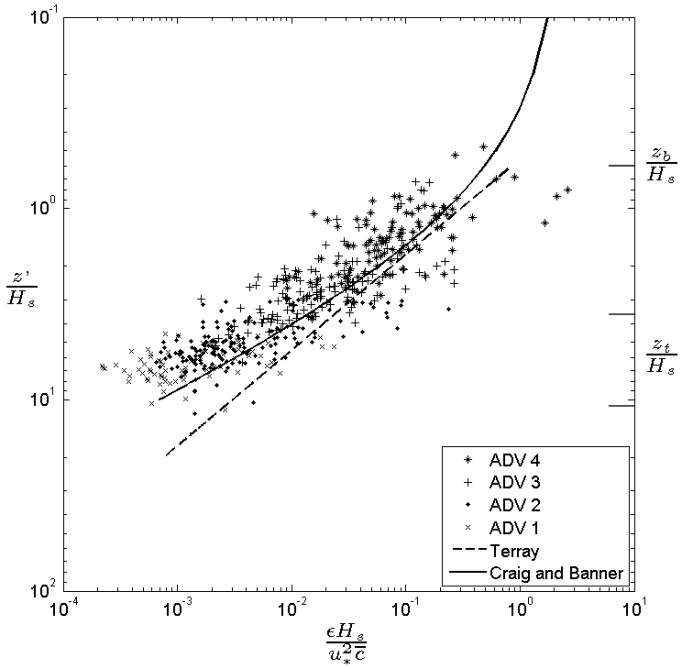

Figure 8 Dissipation normalised using Terray et al. (1996) scaling. z_b and z_t are the length scales of the breaking zone and transition depth to wall layer respectively. Comparisons with the findings of Terray et al. (1996) and Craig and Banner (1994) are shown. The range of z_t is due to the range of $\overline{c}/u_{*a}$ in the experiment

To eliminate the need for calculating the rate of energy input to the waves, employing the use of an expres-

sion for the integral growth rate over the wave spectrum, the Craig and Banner (1994) definition for the kinetic energy flux αu_{*w}^3 can be used and the parameter α, referred to as the wave energy parameter (Craig and Banner 1994), can be found by regression of the data. The α value is known to be dependent on the wave age (c_p / u_{*a}), therefore it will not be a constant for this data set, where the wave age is varying between 4.3 and 12, however, an approximate value can be found. The data were scaled with:

$$\frac{\varepsilon H_s}{\alpha_T u_{*w}^3} = 0.3\left(\frac{z'}{H_s}\right)^{-\beta_T} \quad (8)$$

And the best fit to α_T and β_T were estimated by linear regression (Figure 9). Similarly the Craig and Banner (1994) relationship (Eq. (7)):

$$\frac{\varepsilon z_0}{\alpha_C u_{*w}^3} = 2.4\left(1+\frac{z'}{z_0}\right)^{-\beta_C} \quad (9)$$

can be fit to the data to estimate α_C and β_C.

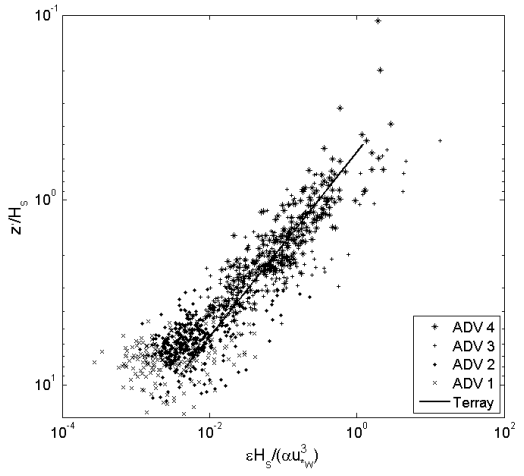

Figure 9 Dissipation scaled using Terray et al. (1996) scaling (with the Craig and Banner (1994) formulation for the kinetic energy flux) with best fit for α=19 and exponent -2

Table 1 displays the estimates of α for the two alternative methods of estimating wind stress from wind velocity. The Donelan (1990) method accounts for the effect of waves and whitecapping on the wind stress, leading to larger stresses for higher wind conditions, compared with the Large and Pond (1981) algorithm for well developed seas. For the Terray et al. (1996) and Craig and Banner (1994) methods for calculating the rate of energy input to the waves from the wind to agree, $\alpha = \overline{c} / u_{*w}$. However, the results show that compared with the range of values of $\overline{c} / u_{*w}$ throughout the experiment (Figure 10) the values of α, estimated by fitting the data set, are smaller in comparison. This indicates that the method for calculating the integral growth rate of the waves is overestimating the energy flux. For comparison Craig and Banner (1994) used a value of α=100 in the model and Feddersen et al (2007) found that α=250 for their nearshore measurements. A low value of the wave energy parameter α implies that the efficiency of energy transfer from the wind to the waves is relatively low at the Grizzly Bay location. This may be due to the shallow water conditions that lead to depth limited breaking that prevents waves growing beyond a certain wave height and period.

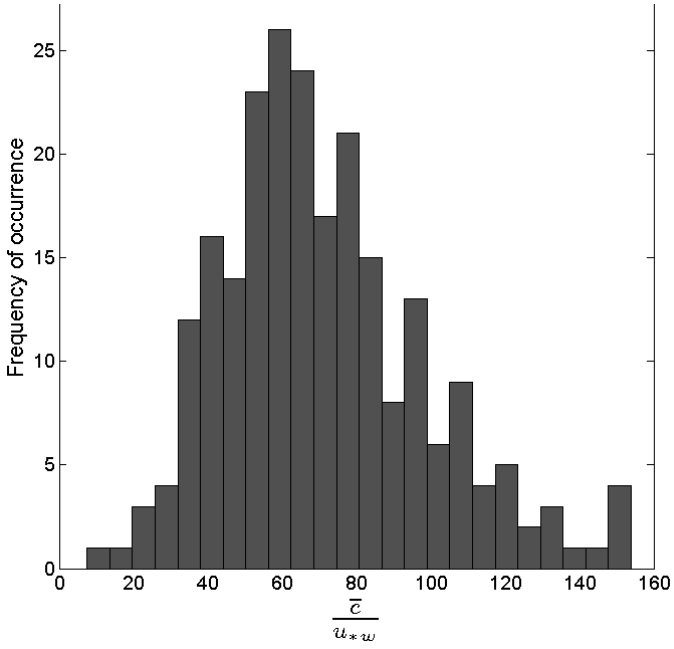

Figure 10 Histogram of $\overline{c} / u_{*w}$ calculated via Eq (4)

If we assume that the log-layer due to the surface wind stress does not exist and that the wave-breaking surface layer directly transitions to the bed stress log-layer, the location of the transition between the two layers can be

calculated. This can be achieved by equating Eq. (1) and Eq. (8) resulting in the transition to breaking wave dominated dissipation being defined as a height above the bed z_{trans}

$$0 = -z_{trans}^{2} + \left(0.3\alpha_T \kappa H_s \frac{u_{*w}^3}{u_{*b}^3} + 2h \right) z_{trans} - h^2 \quad (10)$$

where h is the water depth. Using the measured values of wind and bed stresses and wave height, the roots to Eq. (10) can be found. The value less than the water depth are the physical solutions. If the transition depth is normalized by the total water depth it can be shown that the dominant source of dissipation is frequently wave breaking over the entire water column (Figure 11). This source of turbulence has never been included in models of phytoplankton dynamics. Historical wind records indicate that more occurrences of high wind speed (>5 m/s) occur in the months of August, September and October, with wind directions conducive to the generation of large waves, than occurred during this experiment. The historical wind data suggests that an even higher occurrence of complete penetration of the water column by wave breaking generated turbulence would occur in these months.

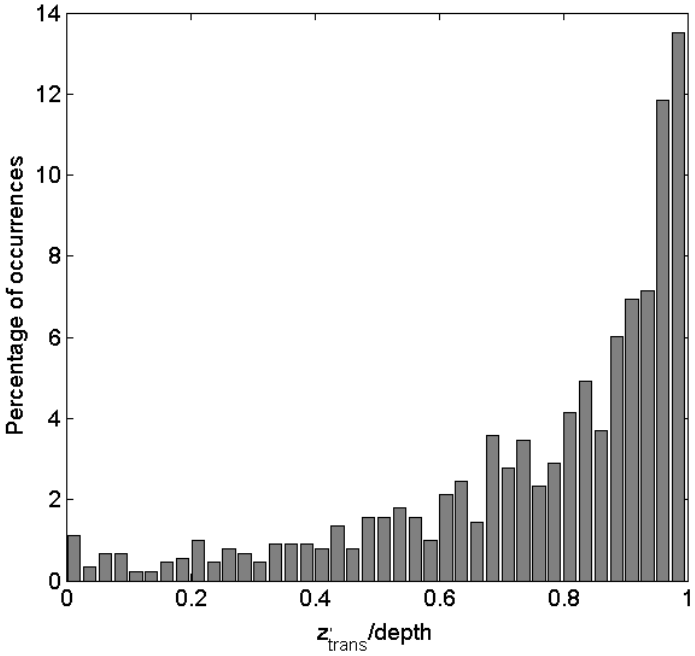

Figure 11 Distribution of normalized penetration depth of surface wave breaking dominance of dissipation.

Table 1 Estimates of α and β parameters from best fit to data from ADV3 and ADV4 to both Terray et al.(1996) and Craig and Banner (1994) formulations using wind stresses estimated via the Donelan (1990) and Large and Pond (1981) methods. The numbers in parenthesis are the 95 % confidence intervals for each estimate.

Wind stress estimation	*Terray et al. (Eq. (8))*		*Craig and Banner (Eq. (9))*	
	α_T	β_T	α_C	β_C
Donelan (1990)	*21.1*	*2.03*	*24.6*	*3.22*
	(19.4-22.9)	*(1.94 -2.12)*	*(20.8-29.3)*	*(3.07-3.36)*
Large and Pond (1981)	*34.7*	*2.04*	*39.3*	*3.21*
	(31.2-38.5)	*(1.92-2.17)*	*(31.5-49.0)*	*(3.02-3.40)*

Conclusions

This data set demonstrates that locally generated, whitecapping, surface waves can influence the distribution and magnitude of turbulent kinetic energy in the water column which will in turn influence the distribution of constituents such as sediment and phytoplankton. Without the incorporation of surface waves effects, numerical models of shallow water bodies, where the bottom boundary layer overlaps with the wave affected surface layer, will not predict the correct distribution of TKE or correct mean current profiles. Therefore, the mixing and transport of constituents such as sediment and phytoplankton will not be predicted accurately.

Many shallow water locations in San Francisco Bay, as well as other estuarine and coastal regions are likely to experience conditions similar to those in Grizzly Bay. The findings of this study are widely applicable. Ultimately, this data set will be used to help us understand the relative importance of the different physical forces in mixing sus-

pended and resuspended sediment particles and phytoplankton in and out of the euphotic and benthic grazing zones, thereby improving the predictive ability of shallow water models.

References

Agrawal, Y. C., E. A. Terray, M. A. Donelan, P. A. Hwang, A. J. Williams, W. M. Drennan, K. K. Kahma, and S. A. Kitaigorodskii. 1992. Enhanced dissipation of kinetic-energy beneath surface-waves. Nature **359:** 219-220.

Alpine, A., and J. Cloern. 1992. Trophic interactions and direct physical effects control phytoplankton biomass and production in an estuary. Limnology and Oceanography **37:** 946-955.

Anis, A., and J. N. Moum. 1995. Surface wave-turbulence interactions - scaling epsilon(z) near the sea-surface. J. Phys. Oceanogr. **25:** 2025-2045.

Bricker, J. D., S. Inagaki, and S. G. Monismith. 2005. Bed drag coefficient variability under wind waves in a tidal estuary. Journal of Hydraulic Engineering-ASCE **131:** 497-508.

Cloern, J. 1996. Phytoplankton bloom dynamics in coastal ecosystems: A review with some general lessons from sustained investigation of San Francisco Bay, California. Reviews of Geophysics **34:** 127-168.

Cohen, R., P. Dresler, E. Phillips, and R. Cory. 1984. The effect of the asiatic clam, corbicula-fluminea, on phytoplankton of the Potomac River, Maryland. Limnology and Oceanography **29:** 170-180.

Craig, P. D., and M. L. Banner. 1994. Modeling wave-enhanced turbulence in the ocean surface-layer. J. Phys. Oceanogr. **24:** 2546-2559.

Dame, R., R. Zingmark, H. Stevenson, and D. Nelson. 1980. Filter feeder coupling between the water column and benthic subsystems, p. xxi, 533. *In* V. S. Kennedy, Estuarine Research Federation. and United States. Environmental Protection Agency. [eds.], Estuarine perspectives. Academic Press.

Donelan, M. A. 1990. Air-sea interaction, p. 239. *In* B. LeMehaute and D. M. Hanes [eds.], Ocean engineering science. The sea, ideas and observations on progress in the study of the seas Wiley.

Drennan, W., M. Donelan, E. Terray, and K. Katsaros. 1996. Oceanic turbulence dissipation measurements in SWADE. J. Phys. Oceanogr. **26:** 808-815.

Feddersen, F., J. H. Trowbridge, and A. J. Williams. 2007. Vertical structure of dissipation in the nearshore submitted to J. Phys. Oceanogr.

Feyrer, F., and M. Healey. 2003. Fish community structure and environmental correlates in the highly altered southern Sacramento-San Joaquin Delta. Environmental Biology of Fishes **66:** 123-132.

Kitaigorodskii, S. A. 1983. On the theory of the equilibrium range in the spectrum of wind-generated gravity-waves. J. Phys. Oceanogr. 13: 816-827.

Kitaigorodskii, S. A., and J. L. Lumley. 1983. Wave turbulence interactions in the upper ocean .1. The energy-balance of the interacting fields of surface wind-waves and wind-induced 3-dimensional turbulence. J. Phys. Oceanogr. 13: 1977-1987.

Large, W. G., and S. Pond. 1981. Open ocean momentum flux measurements in moderate to strong winds. J. Phys. Oceanogr. 11: 324-336.

Lumley, J. L., and E. A. Terray. 1983. Kinematics of turbulence convected by a random wave field. J. Phys. Oceanogr. **13:** 2000-2007.

Nichols, F. 1985. Increased benthic grazing - an alternative explanation for low phytoplankton biomass in northern San Francisco Bay during the 1976-1977 drought. Estuarine Coastal and Shelf Science **21:** 379-388.

Shaw, W., and J. Trowbridge. 2001. The direct estimation of near-bottom turbulent fluxes in the presence of energetic wave motions. Journal of Atmospheric and Oceanic Technology **18:** 1540-1557.

Soloviev, A., and R. Lukas. 2003. Observation of wave-enhanced turbulence in the near-surface layer of the ocean during toga coare. Deep-Sea Research, Part I (Oceanographic Research Papers) **50:** 371-395.

Tennekes, H., and J. Lumley. 1972. A first course in turbulence MIT Press.

Terray, E. A., M. A. Donelan, Y. C. Agrawal, W. M. Drennan, K. K. Kahma, A. J. Williams, P. A. Hwang, and S. A. Kitaigorodskii. 1996b. Estimates of kinetic energy dissipation under breaking waves. Journal of Physical Oceanography **26:** 792-807.

Thompson, J. K. 1999. The effect of infaunal bivalve grazing on phytoplankton bloom development in south San Francisco Bay. Stanford University Press.

Trowbridge, J., and S. Elgar. 2001. Turbulence measurements in the surf zone. Journal of Physical Oceanography **31:** 2403-2417.

Wildish, D., and D. Kristmanson. 1984. Importance to mussels of the benthic boundary-layer. Canadian Journal of Fisheries and Aquatic Sciences **41:** 1618-1625.

■ Interagency Ecological Program for the San Francisco Estuary ■

IEP NEWSLETTER

3251 S Street
Sacramento, CA 95816-7017

For information about the Interagency Ecological Program, log on to our website at http://www.iep.water.ca.gov. Readers are encouraged to submit brief articles or ideas for articles. Correspondence—including submissions for publication, requests for copies, and mailing list changes—should be addressed to Patricia Cornelius, California Department of Water Resources, P.O. Box 942836, Sacramento, CA, 94236-0001. Questions and submissions can also be sent by e-mail to: pcorn@water.ca.gov.

■ Interagency Ecological Program for the San Francisco Estuary ■

IEP NEWSLETTER

The Interagency Ecological Program for the San Francisco Estuary
is a cooperative effort of the following agencies:

California Department of Water Resources
State Water Resources Control Board
U.S. Bureau of Reclamation
U.S. Army Corps of Engineers
California Department of Fish and Game
U.S. Fish and Wildlife Service
U.S. Geological Survey
U.S. Environmental Protection Agency

National Marine Fisheries Service

BEFORE CITING INFORMATION HEREIN,
CONSIDER THAT ARTICLES HAVE NOT RECEIVED PEER REVIEW.